Study of spatially extended dynamical systems using probabilistic cellular automata

V K Vanag

Contents

Abstract. Spatially extended dynamical systems are ubiquitous and include such things as insect and animal populations; complex chemical, technological, and geochemical processes; humanity itself, and much more. It is clearly desirable to have a certain universal tool with which the highly complex behaviour of nonlinear dynamical systems can be analyzed and modelled. For this purpose, cellular automata seem to be good candidates. In the present review, emphasis is placed on the possibilities that various types of probabilistic cellular automata (PCA), such as DSMC (direct simulation Monte Carlo) and LGCA (lattice-gas cellular automata), offer. The methods are primarily designed for modelling spatially extended dynamical systems with inner fluctuations accounted for. For the Willamowski – Rössler and Oregonator models, PCA applications to the following problems are illustrated: the effect of fluctuations on the dynamics of nonlinear systems; Turing structure formation; the effect of hydrodynamic modes on the behaviour of nonlinear chemical systems (stirring effects); bifurcation changes in the dynamical regimes of complex systems with restricted geometry or low spatial dimension; and the description of chemical systems in microemulsions.

V K Vanag Center for Photochemistry, United Institute of Chemical Physics, Russian Academy of Sciences,
ul Novatorov 7A, 117421 Moscow, Russian Federation
Tel. (7-095) 932 03 90
Fax (7-095) 936 12 55
E-mail: Vanag@photch.chemphys.msk.su;
    Vanag@binah.cc.brandeis.edu

1. Introduction

1.1 What are cellular automata (CA)?

The history of automata probably goes back to the 60's when M L Tsetlin and his colleagues published their papers on the subject [1 – 7]. Modelling advisable behaviour of biological systems in an environment, i.e. behaviour allowing a system to adapt to an environment, Tsetlin introduced a mathematical notion which received the name *automaton* or *finite automaton*. The adjective *finite* means that the automaton can only be in a finite number of states. It can perceive a finite number S of signals from the environment (as a rule, $S = 0$ or $S = 1$) at discrete moments $t = 1, 2, \ldots$, as a result of which its state changes. And finally, the automaton can execute a finite number of actions unambiguously determined by the state of the automaton. The actions of the automaton provoke a response S of the environment, closing a feedback loop. In deterministic automata the signal S determines exactly a state j to which the automaton transits from the state i. In probabilistic automata the transition is given by certain probabilities $a_{ij}(S)$.

The works of American mathematician J von Neumann on the theory of automata games were the addition to the theory of isolated finite automata. Trying to model the self-replication of biological systems, in 1966 von Neumann invented abstract discrete dynamical systems, which were given the name *cellular automata* (CA). A cellular automaton [9 – 13] consists of a set of nodes (cells) forming a regular lattice. A node (or cell) is characterised by a discrete set of integer variables, which can have a finite number of values. The cell variables change simultaneously at discrete moments, following deterministic or probabilistic rules, which can

depend on the values of variables in the neighbouring cells. The rules do not change in time.

Comparing CA and ordinary differential equations (ODE), the main difference between them is that in the case of CA the rules describing the dynamics of a system are local. Whereas applying ODE, we are dealing with the rules for dynamic changes of quantities averaged over the system, i.e. averages (for instance, concentrations). Hence we believe *a priori* the rules to exist. In the case of CA the existence of such generalised rules (or macrorules) is not required. It is sufficient to know the rules for dynamic changes in small micro- or mesoscopic regions (cells) of which the system consists. What matters is only that the local rules be the same for all the cells. Another difference of CA from differential equations (DE) is that the cell variables are not only discrete but also integer. Discreteness of variables enables one to consider a large group of discontinuous nondifferentiable functions. It should be mentioned that the discrete properties of CA are less pronounced when the values of variables are large, however they never disappear. There is always a minimal discrete step for changing a variable. Whereas in the case of ODE or DE in partial derivatives the magnitude of the step can be decreased down to indefinitely small values.

The local character of dynamic rules and the discreteness of variables in the case of CA allow one to take into account fluctuations or internal noise of the system in a natural way without any additional assumptions. To consider fluctuations in the case of DE one should use stochastic DE and apply various fluctuation-dissipation relations to solve them. The latter may be rather a cumbersome procedure [14].

Sometimes a combination of such properties as local rules and discreteness of variables results in unexpected behaviour of a spatially extended discrete system. Unexpected behaviour (not to be confused with chaotic behaviour!) is an additional feature of CA, the term being used here to characterise mainly qualitative aspects of the behaviour. There are a large number of papers devoted to CA (see, for example, Refs [9 – 13, 15 – 35]). Some works deal with the mathematical properties of abstract CA [9 – 12, 16, 20, 26, 28, 32, 36 – 42]. Others consider detailed behaviour of certain reaction-diffusion equations [15, 22 – 25, 29, 30, 33 – 35, 43 – 50].

1.2 What are CA needed for?
The main peculiarities of a complicated dynamical system can often be described by simple rules. The desire to reveal the simplest local rules underlying the behaviour of a complicated dynamical system accounts for much favour held by CA. The problem is similar in a sense to the inverse problem of chemical kinetics which is to determine the rules underlying the behaviour of a system from the data on its functioning in time.

CA are most effectively used to describe various phase or bifurcation transitions, when fluctuations must be taken into account, or when cooperative behaviour of the system is determined by local behaviour of its elements. They are also suited to consider the transition processes when the system becomes highly heterogeneous and one can hardly find any averages, relevant to determine the state of the system. To illustrate the application of CA for the investigation of complicated systems we point out the following cases. CA are used to analyse fingerprints [42, 51], to describe phase transitions in physico-chemical systems [52], to analyse the

'free motion – jam' transitions occurring in cities [53], to investigate the formation of various structures (for example shell patterns of sea molluscs and zebra strias) [26, 41, 54], to consider the collective motion of organisms (bees, slugs, birds, etc.) [19], to find the optimal path for searching numerous distributed objects [32], and in many other cases [18].

Probabilistic CA are applied to a wide range of problems concerned with the influence of fluctuations on the behaviour of nonlinear dynamical systems with critical or bifurcation points. These problems are traditionally solved with the use of a master equation and the Langevin equation (see, for example, [55]). However an analytical solution to the equations can be found only in a few special cases, such as simple 'point' systems consisting of one or two variables. The application of the master equation to spatially extended systems of the 'reaction – diffusion' type is well known [43, 56 – 60] but presents great mathematical difficulties.

When dealing with reaction – diffusion – convection problems where fluctuations must be taken into account traditional approaches are unsuitable. In this case some special CA are applied. They will be described in detail in Sections 6 – 8. Here we only indicate that in describing turbulent motion use is made of the models of cells or CA, where each cell represents a microelement of fluid (coarse grained structure of fluid) [61 – 63].

1.3 Types of CA
CA can be classified as deterministic and probabilistic, homo- and heterogeneous (the latter can describe fractal structures), simple abstract and complicated ones applied to describe detailed behaviour of actual systems. The classification can be based on some other criteria as well. For example, Gutowitz [41, 42] divides CA into two groups, i.e. those functioning on infinite and finite lattices. In deterministic CA the state of a cell at each moment is unambiguously determined by the state of this cell and its neighbours at the previous moment. Such CA are referred to as *simple* or *classical* ones. Sometimes CA are described by rules written as ordinary differential equations. In this case the states of cells are determined by a set of variables, whose values can be any real numbers. The differential equations are solved for each cell separately during a certain period Δt, each cell being able to have various initial conditions. We will designate such CA as *CA-ODE*. This type of CA is closely related to DE in partial derivatives.

CA, where the states of the cells at each moment of time are determined by probabilities, are called *probabilistic CA* (PCA) [64, 65]. In the classical PCA the rules of transitions are abstract and not related directly to actual processes occurring in the system under study. In the past decade considerable study has been given to CA, in which the probabilities of transitions are straightforwardly derived from the processes under consideration, for example, from diffusion processes or real chemical reactions. In modelling or simulating a process, a randomiser generates a random number θ $(0 < \theta < 1)$ for each cell of the CA, which is compared with the probability W of occurrence of the process. When $\theta < W$, the process takes place. The examples of CA of this type are the method of reactive lattice gas (LGCA), direct simulation by Monte Carlo (DSMC), and the method of probabilistic CA using the Monte Carlo procedure. All the methods and ways for obtaining W will be described below.

The methods of complete molecular dynamics (MD), where the dynamics of all the particles of the system are studied, can also be assigned to CA. Such investigations are cumbersome and therefore deal with a small number of particles considering them in a small spatial region over a short time interval. There are some examples of the application of MD to systems far from equilibrium [66–68]. The LGCA, DSMC, and PCA models are intermediate between complete MD and macroscopic description with the use of reaction–diffusion equations such as CA-ODE and DE in partial derivatives.

2. Simple or classical CA

As indicated above, the main problem of the description of a macrosystem by CA is to find local rules for the elements of the system, which would enable the ensemble of elements to reproduce the evolution of the phenomenon under consideration. Looking over a multitude of the rules for simple CA (the number of various CA is of the order of $(k^k)^d$, where k is the number of various states of an elementary cell, and d is the number of neighbours), Chate and Manneville [69] demonstrated that the global behaviour of some CA is not directly related to the local dynamics of the CA constituents (this is a manifestation of the unpredictability of CA). The question arises as to how we can find the local rules for the system constituents such that the ensemble of the constituents reproduces the desired dynamics of the system? The answer still remains unclear.

Classifying CA by their behaviour, Wolfram [10–12] sets off four groups of CA. The first group includes CA which, irrespective of the initial configuration, arrive eventually (in a finite number of steps) at a homogeneous configuration. The second group contains CA, which in the course of evolution generate simple periodical structures for any initial configurations. CA of the third group produce chaotic structures varying in time. The appearance of the structures follows some statistics, which are independent of the initial conditions. It can be said that the deterministic chaos generated by these CA wipes off the memory of the initial conditions. The last group includes CA which can generate travelling soliton-like structures. The behaviour of these CA depends on the initial configuration of the system, therefore they can be used to produce memory units for computer calculations. These CA do not follow mean-field statistics, their collective behaviour is not a mere 'sum of the evolution' of the elements of the system. This classification is purely phenomenological, it does not provide any recipes for the construction of appropriate rules of CA evolution. Some other phenomenological criteria of classification of numerous rules for evolution of simple CA are also available [70–72].

Classical CA are used in problems of signal filtration [73], in cryptography [51], in problems of crystal formation, in the study of processes of aggregation and cluster formation [74], and in many other fields. However, our main interest is to describe the kinetics of complicated chemical reactions with due regard to diffusion and convection. As a rule, the exact quantitative solution of such problems is found with the use of complicated probabilistic CA. We will consider them in detail in Sections 4–8. Nevertheless, sometimes simple CA allow one to explain qualitatively the dynamics of such systems [14, 75–79].

An example of the application of simple CA to the reaction–diffusion problems is the model developed by Oono and Kohmoto [75–78] where each cell of the automaton, if it is not connected with neighbouring cells, is governed by cyclic dynamics, moving in time around the circle $0 - M - 1 - 0$, where M is a positive number.

To investigate a two-dimensional variant of such CA, we write the symbol $A(i, j, t)$ for the state of a cell with spatial coordinates i and j at the moment t. The variable $A(i, j, t)$ can take one of the three values 0, 1, and M, and evolves as:

$$A(i, j, t + 1) = F\bigl(\bar{A}(i, j, t)\bigr),$$

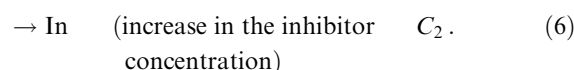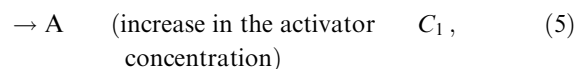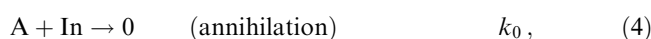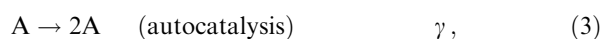$$\bar{A}(i, j, t) = \alpha \sum_{(k, l) \in O} \frac{A(k, l, t)}{N} + (1 - \alpha) A(i, j, t), \tag{1}$$

where the symbol O denotes the nearest vicinity of the cell with coordinates i and j, while N is the number of cells in the vicinity. In the case of a rectangular lattice O can be taken to include four neighbouring cells having a common face with the cell under consideration, or eight neighbouring cells having common nodes. The parameter α characterises the diffusion coefficient (the greater is the diffusion coefficient, the higher is the parameter $\alpha \in [0, 1]$),

$$F(x) = \begin{cases} 1, & \text{if} \quad 1.5 \leqslant x, \\ 0, & \text{if} \quad 0.5 \leqslant x < 1.5, \\ M, & \text{if} \quad x < 0.5. \end{cases} \tag{2}$$

Depending on the parameters M and α the automaton of Oono and Kohmoto can fall into one of Wolfram's classes. The studies of the two-dimensional variant at various M and α revealed spiral waves or moving objects like the gliders in the game 'Life' (the rules for the game 'Life' are considered in Ref. [80]). In the one-dimensional case, waves which annihilate upon collision or are reflected by each other were found [75–77].

As an example of simple but probabilistic CA applied to the reaction–diffusion–convection problems we consider an activator–inhibitor system. In Refs [14, 79], the system included the following reactions:

$A \to 2A$	(autocatalysis)	$\gamma,$	(3)
$A + In \to 0$	(annihilation)	$k_0,$	(4)
$\to A$	(increase in the activator concentration)	$C_1,$	(5)
$\to In$	(increase in the inhibitor concentration)	$C_2.$	(6)

Under the condition $C_1 > C_2$ these reactions adequately represent autocatalytic growth of the activator A in the well known oscillating reactions such as Belousov–Zhabotinskiĭ (BZ) reaction or Briggs–Rauscher (BR) reaction. The system of ODE describing reactions (3)–(6), suggests that when the concentration of the inhibitor [In] decreases to the critical one:

$$[\text{In}]_{\text{cr}} = \frac{\gamma}{k_0}, \tag{7}$$

the concentration of the activator begins to increase autocatalytically in a homogeneous system with good stirring.

The simplest PCA is a one-parametric model, where the state of each cell is characterised only by an integer number S together with integer coordinates i and j. In modelling the activator–inhibitor system the number S can be related to the

ratio between the concentrations [A] and [In]: the larger S, the higher [A] and the smaller [In]. Let us consider the ways for describing diffusion, turbulent stirring, and chemical reactions. Diffusion can be treated in two different ways depending on the spatial scale assigned to an elementary cell. If the cell is believed to be rather large and includes a lot of particles (hundreds, thousands and more), the influence of fluctuations can be ignored. In this case diffusion mixing between neighbouring cells can be described by the averaged formula [14]

$$S_1(t+1) = S_2(t+1) = \frac{S_1(t) + S_2(t)}{2}, \quad (8)$$

where $S_1(t+1)$ and $S_2(t+1)$ are the states of two adjacent cells at a discrete moment $t+1$.

In the opposite case when the cell is of nanosize and contains only few particles (perhaps, zero), diffusion should be described in a probabilistic manner as follows. Let us determine a probability $W(S_1, S_2 | S_1', S_2')$ that at the moment $t+1$ the states of two randomly chosen neighbouring cells are S_1' and S_2' under the conditions $S_1 + S_2 = S_1' + S_2'$, where S_1 and S_2 are the states of these cells at the moment t. In determining $W(S_1, S_2 | S_1', S_2')$ one can proceed from either of two different views of mass exchange. According to the first one [79, 81], the number of particles in a cell may change by no more than one as a result of mass exchange between neighbouring cells (one-step model). Within the other approach [33, 34] the number of particles may change arbitrarily. What matters is only that the final distribution of the cells over the states coincides with the corresponding equilibrium distribution, which is the Poissonian or binomial in most cases. In our consideration we are dealing with the one-step model. According to the model, the probability $W_-(S_1, S_2)$ that as a result of mass exchange the state S_1 will decrease by one and the state S_2 will increase by one is determined as

$$W_-(S_1, S_2) = W(S_1, S_2 | S_1 - 1, S_2 + 1)$$

$$= \frac{S_1}{S_1 + S_2}\left(1 - \frac{S_2}{S_{max}}\right). \quad (9)$$

The probability $W_+(S_1, S_2)$ of the inverse process is determined in a similar way

$$W_+(S_1, S_2) = W(S_1, S_2 | S_1 + 1, S_2 - 1)$$

$$= \frac{S_2}{S_1 + S_2}\left(1 - \frac{S_1}{S_{max}}\right), \quad (10)$$

where S_{max} is the maximum number of particles in a cell. In the limit $t \to \infty$ we get an equilibrium binomial distribution of the cells over the states. The intensity of the diffusion is given by the number $ND \times N_0$ of randomly chosen pairs of neighbouring cells per unit time, where ND is a real number, while N_0 is the total number of cells in the automaton. Varying ND (for example, from 0 to 1), we can regulate the intensity of the diffusion over a wide range.

Turbulent motion can be considered as a combination of turbulent pulsations of various scales [82]. At small Reynolds numbers Re the system exhibits only large-scale pulsations, comparable with the size of the system. As Re rises, the scale of pulsations progressively decreases. To model the large-

scale pulsations on the basic lattice of size $N \times N$ (for example, $N = 2^8$, $N_0 = N \times N$), squares of size $\lambda_n \times \lambda_n = 2^n \times 2^n$, where $n = 7$, were chosen randomly. After that four quadrants of each chosen square were rearranged randomly. An increase in the intensity of stirring was simulated by successive additions of progressively reduced scales of turbulent motion, i.e. by additional selection of squares with side $\lambda_n = 2^n$, where $n = 6, 5, \ldots, 1$, and corresponding rearrangement of their quadrants (Fig. 1). The numbers N_n of samples of squares with side λ_n in a unit time were fitted so that the velocity of the motion of a fluid element should satisfy the Kolmogorov – Obukhov law for each scale of the motion [82]. It was found in Ref. [14] that $N_n \cong 2^{8(7-n)/3}$. Figure 2 plots patterns of turbulent stirring for a black square. It is seen that in four steps the black square is divided into a huge number of small fragments filling the whole of the volume.
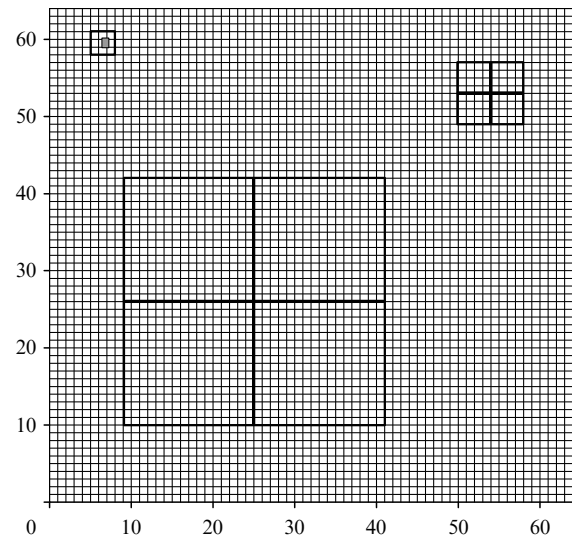

Figure 1. Lattice containing 64×64 elementary cells. The large and middle squares divided into four quadrants are examples of squares used to model turbulent stirring, their quadrants are randomly rearranged. The rearrangements of large quadrants correspond to large-scale vortices, while those of small quadrants represent small-scale vortices. The smallest quadrant of size 3×3 with the central dashed cell represents the vicinity of the cell, used to treat the diffusion process.

To simulate chemical reactions (3) and (4) the authors of Refs [14, 79] use the probabilities $W_+(S)$ that the number of particles S increases by one and $W_-(S)$ that this number decreases by one:

$$W_+(S) = \frac{1}{1 + \exp(2 + S_{cr} - S)}, \quad (11)$$

$$W_-(S) = \frac{1}{1 + \exp[2 + 2(S - S_{cr})]}. \quad (12)$$

At $S < S_{cr}$ the annihilation reaction (4) is dominant, i.e. $W_+(S) < W_-(S)$, while at $S_{cr} < S$ the autocatalytic reaction (3) is dominant, i.e. $W_-(S) < W_+(S)$. The state S_{cr} corresponds to the critical concentration of inhibitor $[In]_{cr} = \gamma/k_0$ (7). When the state of i cell is equal to S_{max}, then the probability $W_+(S)$ is believed to be zero. The probabilities of reactions (5) and (6) are given by constants W_+ and W_-
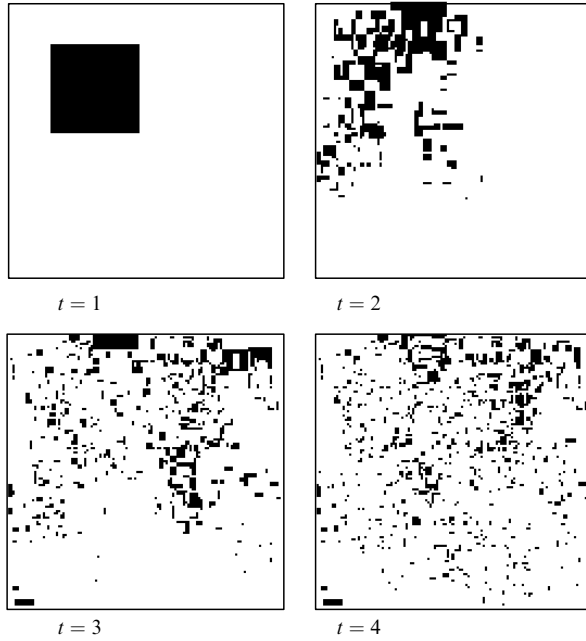
Figure 2. Patterns arising on a lattice $N \times N = 2^8 \times 2^8$ at moments $t = 1, 2, 3, 4$ when a black square including 80×80 elementary cells is mixed barring diffusion ($ND = 0$). The intensity of stirring is characterised by the size of the smallest randomly chosen square with the side $\lambda_n = 2^3$ (Lev $= 8 - 3 = 5$).

independent of the state of the cell S:

$$W_+ = \frac{N_1}{N_0} < 1 \,, \qquad W_- = \frac{N_2}{N_0} < 1 \,. \tag{13}$$

The number N_1 (N_2) stands for the number of randomly chosen cells in which the state S increases (decreases) by one due to the action of the activator (inhibitor) source, $N_1/N_2 = C_1/C_2$.

All probabilistic processes were realised as follows. The probabilities W were calculated by (9)–(13) for each cell and for each pair of neighbouring cells in the case of diffusion. After that a randomiser generated a number $\theta \in [0, 1]$ for each W and each cell. If the inequality $\theta < W$ was satisfied, the process corresponding to the probability W occurred, otherwise it did not. Molecular diffusion, chemical reactions, and turbulent stirring were modelled successively in a unit time interval. In the course of computer simulation one could follow, in particular, the function $p(S)$ of the distribution of the cells over the states S, the mean state of the cells $\langle S \rangle$, and the dispersion σ^2:

$$p(S) = \frac{N(S)}{N_0} \,, \tag{14}$$

$$\langle S \rangle = \sum_{S=S_{\min}}^{S_{\max}} S \, p(S) \,, \tag{15}$$

$$\sigma^2 = \sum_{S=S_{\min}}^{S_{\max}} \left(S - \langle S \rangle \right)^2 p(S) \,, \tag{16}$$

where $N(S)$ is the number of cells in the state S (the cell histogram).

When the diffusion coefficients are not too high, the simulation yields a typical time dependence $\langle S \rangle$ which is in good agreement with actual kinetics of the BZ and BR reactions [14]. After an induction period T_{ind}, a rapid

exponential increase in $\langle S \rangle$ takes place, changing to linear growth, then the system reaches the limiting value $S_{\max}$. In this case the dependence of T_{ind} on the intensity of stirring has an S-like shape. However for more intensive mass exchange and stirring the autocatalysis may fail to occur which is inconsistent with either model (3)–(6) or experiment. This suggests that the one-parametric model determined by (9)–(13) may be inadequate for the two-parametric model (3)–(6).

The advantages of simple PCA models are the quickness of their calculations and sound qualitative results consistent with the experiment. The above-discussed model has allowed us to describe qualitatively some experimental facts such as the S-like dependence of the induction period on the intensity of stirring, and the dependence of the value of the stirring effect on the rate at which the system approaches the critical point determined by the difference $W_+ - W_-$. However neither this model, nor any other simple models of CA reveal a direct relation between ND (or its analogue) and the actual coefficient of molecular diffusion, and between the functions of type (11)–(13) and the probabilities of the occurrence of actual chemical reactions. Time is a conventional quantity in the model and cannot be related to the actual duration of the process concerned. All these drawbacks do not enable one to be sure that simple CA are adequate.

To conclude the section we will show how simple CA can be used to model reactions on irregular lattices of fractal dimension. As an example we consider the lattice depicted in Fig. 3, referred to as the *Sierpinski carpet*, which is formed from a basic matrix of size 3×3, containing only 0 and 1. If we choose the basic matrix in the form

$$\begin{array}{ccc} 1 & 1 & 1 \\ 1 & 0 & 1 \\ 1 & 1 & 1 \end{array} , \tag{17}$$

replace all the unity elements in it by the basic matrix, and all the zero elements by the zero matrix of the same size 3×3, we get the Sierpinski carpet of size 9×9 plotted in Fig. 3. This expanding procedure can be repeated as many times as one likes. Each unity element in the final matrix obtained in this way means that the place is occupied by a particle, the zero elements cannot be occupied by any particles. Occupied
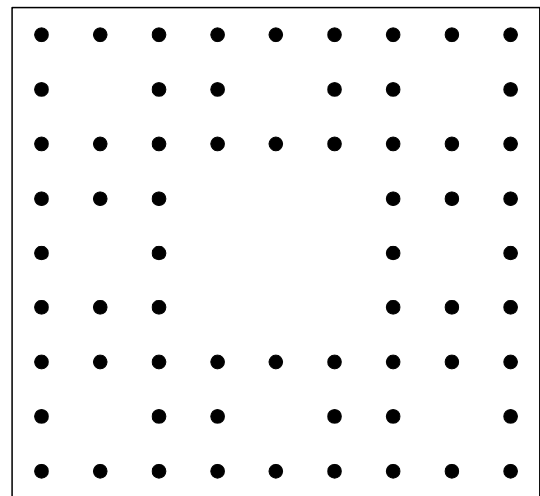

Figure 3. Sierpinski carpet. Each point is occupied by a particle X or A.

elements separated by a minimal distance are called *neighbours*. For example, the nodes with coordinates $(3,3)$, $(3,4)$ and $(3,5)$ in Fig. 3 have 4, 3, and 2 neighbours respectively. The basic matrix can be chosen to have a different number and arrangement of zero and unity elements.

The Sierpinski carpet was used as a lattice to model various chemical systems [83, 84]. An interesting result was obtained in modelling the reaction

$$A + 2X \leftrightarrow 3X,$$
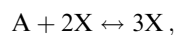
with similar rate constants for the direct and inverse reactions. Modelling on lattices of various configurations, including the Sierpinski carpet, was performed as follows [30, 31, 48, 84]. A lattice node containing either A or X was randomly chosen. If the node had two X neighbours, it changed the state A into X or the state X into A depending on what particle was in the node. It turned out that the equilibrium ratio $\langle A \rangle / \langle X \rangle = K$ was always equal to 1, when the coordination number d (averaged number of neighbours) exceeded 4. When d was less than 4, the equilibrium ratio K also decreased, depending only on d and being almost independent or depending only slightly on the fractal dimension of the lattice. The fractal character of the lattice seems to result only in decreased mobility of the particles and has no other effect on the reaction.

3. CA-ODE (CM)

The main idea of all CA-ODE models is to break down the reaction volume into equivalent cells, and then to solve a set of ODE for each cell individually under various initial conditions. That is why these CA are called 'Cellular models' [85, 86]. In some models the spatial distribution of cells is not essential (the case of turbulent stirring), while in others the number of neighbours and the space dimensionality play a key role (the cases of travelling waves or formation of steady spatial structures in an unmixed medium).

CA-ODE models deal with cells containing a large number of particles so that ODE and continuous functions can be used. This fact leaves only one way for modelling diffusion, namely, a simple averaging of concentrations over neighbouring cells [formulas of the type of Eqn (8)], or over all the cells in the case of turbulent stirring. Strictly speaking, the CA-ODE models are not related to the cell automata, since the states of cells change continuously during the time interval τ (the time of integration of ODE). Therefore we only briefly outline this way of modelling which is also used in coalescence dispersion (CD) models [85 – 88] and in models for interaction by exchange with the mean (IEM) [89 – 92].

Fluctuations are modelled by the replacement of a random number of old cells by new ones with the same initial concentrations (the model of a flow reactor) [93] or by using a randomiser to set the initial concentrations before each step τ of integration (the model of a batch reactor) [94], or by the use of stochastic DE instead of ODE [88].

The CA-ODE models are intermediate between simple CA and PCA as well as between simple CA and DE in partial derivatives. These models allow one to consider external noises and internal fluctuations in actual chemical systems, although the latter is performed in rather an artificial way. The models can be used to simulate reactions at turbulent stirring [85, 86, 93 – 95] and reaction-diffusion spatially extended systems [27].

4. The method of lattice gas cellular automata (LGCA)

The method of reactive lattice-gas cellular automata, (LGCA) [22 – 25, 35, 46, 96 – 98] has been developed to describe spatially extended dynamical systems at the mesoscopic level. It is based on modelling microscopic collisions between particles. Central to the LGCA approach is the Lattice Gas Automaton (LGA) model developed to solve hydrodynamic problems [17, 18, 99 – 102]. The idea of the models is to construct relatively simple dynamic rules which, however, should represent the main essential features of actual collisions between particles and make possible fast simulations in modelling turbulence. Microscopic laws of conservation for mass, momenta, and density of energy, which are the basis of the LGA approach, correspond to the relevant macrorelations involved in the Navier – Stokes equations.

In the LGCA method each node of the lattice with a coordination number d (the number of nearest neighbouring nodes) corresponds to a small region in the actual space and is occupied by interacting particles. Each particle is assumed to have a discrete velocity with unit magnitude and the direction along one of the bonds between neighbours. The spatial coordinates of nodes and time are also discrete quantities. According to LGCA rules, the particles at a node cannot have the same velocity (the analogue of the Pauli principle). This limitation determines the maximum number of particles at the node, which is equal to the coordination number d. The most commonly used lattices have the coordination numbers 3, 4, 6, and 8.

In modelling the diffusion of particles with different diffusion coefficients by the LGCA method use is made of several (k) lattices. On each lattice particles of only one type diffuse. We denote these lattices as L_j $(j = 1, \ldots, k)$, where k is the number of various species of particles. The lattices have the same spatial coordinates, i.e. they are superposed. In each step of time the particles travel a lattice step in the direction determined by their velocities. This propagation step is denoted as operator $\mathbf{P}$. Elastic and inelastic (reactive) collisions are local events which occur only at lattice nodes. Elastic collisions randomly change the direction of motion of a particle. The operator of this event is denoted as $\mathbf{R}$ (random). If the number of particles at a node is α, then the number of possible configurations for the velocities of particles is

$$C_d^\alpha = \frac{d!}{(d-\alpha)! \, \alpha!} . \tag{18}$$

The probabilities of all the configurations are the same. Hence, after a collision of particles in a node the probability of an arbitrary configuration of the velocities will be $1/C_d^\alpha$. The operation $\mathbf{R}$ is carried out independently for each node of all the k lattices.

In the absence of chemical reactions the operation $\mathbf{R}_j \cdot \mathbf{P}_j$ determines the free wandering of particles throughout the lattice L_j. In the long-range limit this operation determines the coefficient D_j of molecular diffusion. Simple calculations [24, 25] demonstrate that for the hexagonal lattice $(d = 6)$ $D_j = D = 1/4$ where D is measured in the units (lattice step)^2/ (time step). If the operation $\mathbf{R}_j \cdot \mathbf{P}_j$ is carried out several times $(m_j$ times) during a time step, the diffusion coefficient may increase m_j times: $D_j = m_j D$. It should be noted that the free

wandering of particles throughout a lattice is not absolutely independent of other particles, since two particles at a node cannot have the same velocity. In view of reaction changes the collisions between particles cannot be considered to be independent either. Actually, as a new particle with a certain velocity arises at a node other particles cannot have the same velocity. However if inelastic collisions are rare, the effect can be ignored.

Inelastic collisions which change the number of particles and their velocities couple the diffusive dynamics on various lattices L_j. The operator $\mathbf{C}$ of chemical changes determines the probability of a reaction, i.e. the probability that the number α_j of particles of X_j species will change into the number β_j of particles of the same species. The operator $\mathbf{C}$ is completely determined by the probability matrix $P(\alpha|\beta)$ for changes from the configuration α of reacting particles to the configuration β of products, where $\alpha = \{\alpha_1, \ldots, \alpha_k\}$, $\beta = \{\beta_1, \ldots, \beta_k\}$. The matrix $P(\alpha|\beta)$ determines the probability for a local reaction to occur

$$\alpha_1 X_1 + \ldots + \alpha_k X_k \rightarrow \beta_1 X_1 + \ldots + \beta_k X_k. \tag{19}$$

The LGCA method deals with the case when indices α change by unity, or more exactly, by the difference of stoichiometric coefficients, following the mechanism of chemical reactions. Diagonal elements of the matrix $P(\alpha|\beta)$ are equal to the probability for a reaction not to take place at a given node and during a given time interval. In a more recent version of the LGCA method [25] the limitation on the number of particles at one node is removed. In this case for reaction (19) or the reaction

$$v_{\mathrm{r}}^i \mathbf{X} \Longleftrightarrow v_{\mathrm{p}}^i \mathbf{X}, \qquad k_i, k_{-i}, \tag{20}$$

where $\mathbf{X} = (X_1, X_2, \ldots, X_k)$ is the vector of k chemical particles, v_{r}^i and v_{p}^i are the vectors of stoichiometric coefficients for reagents and products, while k_i and k_{-i} are the rate constants for direct and back reactions, and the symbol i $(i = 1, 2, \ldots, n)$ denotes the numbers of various elementary reactions, the matrix $P(\alpha|\beta)$ is determined by birth-and-death processes as

$$P(\alpha|\beta) = \tau \sum_{i=1}^{n} \left\{ k_i \prod_{j=1}^{k} \left[\frac{\alpha_j!}{(\alpha_j - v_{\mathrm{r},j}^i)!} \, \delta(\beta_j, \alpha_j + v_{\mathrm{p},j}^i - v_{\mathrm{r},j}^i) \right] \right.$$
$$\left. + k_{-i} \prod_{j=1}^{k} \left[\frac{\alpha_j!}{(\alpha_j - v_{\mathrm{p},j}^i)!} \, \delta(\beta_j, \alpha_j - v_{\mathrm{p},j}^i + v_{\mathrm{r},j}^i) \right] \right\}. \tag{21}$$

The parameter τ is chosen so that all the elements of the matrix $P(\alpha|\beta)$ do not exceed 1. Formula (21) only represents the fact that reactions occur following the reaction mechanisms and the probabilities of their occurrence are proportional to the rate constants and the number of particles at the node. The Kronecker symbol $\delta(\beta_j, a_j + v_{\mathrm{p},j}^i - v_{\mathrm{r},j}^i)$ indicates that the final configuration of particles β has to correspond to the stoichiometry of the reaction.

As was shown in Refs [103 – 105], the LGCA methods yield the correct spectrum of fluctuations in equilibrium systems. The LGCA method was used to investigate the influence of fluctuations on travelling chemical waves and growth of nuclei in bistable chemical systems [22], on the behaviour of excitable media and formation of Turing structures [23, 46], on processes of heterogeneous catalysis, and on oscillatory and chaotic behaviour of chemical systems [24, 25, 35].

In conclusion we note that the LGCA method is based on the calculation of the total probabilities for the number of particles to change in all the reactions in which these particles are involved. The approach gives rather cumbersome expressions for the probability matrix $P(\alpha|\beta)$, when the system contains several reactions and when one and the same particle is involved in more than one reaction. A different approach is developed in DSMC and PCA methods which deal with the probabilities for individual reactions to occur instead of calculation of the total change in the number of particles.

5. The method of direct simulation by Monte Carlo (DSMC)

In the DSMC method [15, 43, 57, 106 – 116] reacting particles are considered as a rare gas consisting of hard spheres (a Boltzmann gas). A computer algorithm for describing such a system was proposed by Bird [109, 111]. It turned out that the DSMC method enables one to model reaction – diffusion equations and agrees well with the experimental data [109, 110, 112, 116] and the data obtained by complete molecular dynamics simulations.

The DSMC method is detailed in Refs [111, 113]. Here we only briefly outline the main features of the method. Initially all the particles considered as spheres are sorted over all the spatial cells, whose linear size l is comparable with the mean free path λ. Time changes by a discrete step τ comparable with the mean time interval between collisions. The cells are assumed to be homogeneous, which means that all the particles inside a cell irrespective of their positions, have the same probability of colliding. This key assumption allows one to decrease the time of calculations by three orders of magnitude with respect to that in molecular dynamics simulations. Note that the cells are equivalent to the so-called maximum volumes of complete mixing (MVCM) introduced by Yu M Romanovskiĭ [117] and similar to the indefinitely small volumes of the Boltzmann gas, considered by Yu L Klimontovich [55, 118].

In practice researchers deal with a number of particles of the order of 10^5, distributed over 10^2 cells [15, 43]. All the particles are assumed to have the same mass m and diameter d; $m = d = 1$. The velocities of particles and temperature are also taken to be unity. The density of the particles (of the order of 10^{-2} per volume d^3) is specified, and the length λ of free flight motion is evaluated for elastic collisions (for example, $\lambda \cong 100d$). Then the diffusion coefficient D and the frequency v of collisions (in dimensionless units) are calculated. The DSMC method only deals with bimolecular reactions. For the reaction

$$\mathrm{X} + \mathrm{Y} \rightarrow \mathrm{products}, \qquad k_1, \tag{22}$$
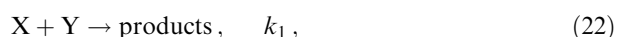
the rate is assumed to be proportional to the constant c_1 determined as

$$c_1 = v k_{1,\mathrm{r}}, \tag{23}$$

where v is the frequency of collisions, and $k_{1,\mathrm{r}}$ is the fraction of inelastic collisions. The constant c_1 has the dimensionality s^{-1} and can be considered as the frequency of inelastic collisions. The specified fraction of inelastic collisions for all the reactions determines completely the whole system. It was shown [43] that in order to receive correct data coinciding with the solution to the master equation, the cell size l should

be equal to the length λ of free flight motion with regard to the reactive collisions. For example, if in the case of a very fast reaction the fraction of inelastic collisions is equal to 0.5 or 0.2, then $l = 2\lambda$ or $l = 5\lambda$, respectively.

The constants c_1 and bimolecular constants k_1 usually used in chemical kinetics relate [119 – 121] as

$$c_1 = \frac{k_1}{V N_A} , \tag{24}$$

where V is the homogeneous reaction volume with complete mixing (cell volume), while N_A is the Avogadro number. For a reaction of the type

$$X + X \rightarrow \text{products} , \quad k_2 , \tag{25}$$
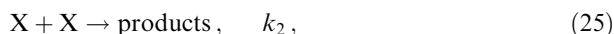
the relation between k_2 and c_2 is given by

$$c_2 = \frac{2 k_2}{V N_A} . \tag{26}$$

Now we only have to determine how the discrete time step τ should be specified and in what sequence the chemical reactions should take place if there are several reactions. To do this we should specify the function $P(\tau, \mu)$ of the probability density, determining the probability $P(\tau, \mu)\,\mathrm{d}\tau$ for the μth reaction (where $\mu = 1, 2, \ldots, n$) to occur in the volume V during indefinitely small period $(t + \tau, t + \tau + \mathrm{d}\tau)$. The probability density $P(\tau, \mu)\,\mathrm{d}\tau$ is given [120] by

$$P(\tau, \mu) = a_\mu \exp(-a_0 \tau) , \tag{27}$$

where $a_\mu = N_X N_Y c_1$ if the μth reaction is of the type of (22) and $a_\mu = N_X(N_X - 1)c_2/2$ if the μth reaction is of the type of (25), N_X and N_Y are the numbers of particles X and Y in the volume V,

$$a_0 \equiv \sum_{i=1}^{n} a_i . \tag{28}$$

Note that $P(\tau, \mu)$ depends on all the rate constants and the numbers of reacting particles.

The procedure of searching for the interval τ after which the μth reaction occurs is based on the transformation

$$P(\tau, \mu) = a_\mu \exp(-a_0 \tau) = P_1(\tau) P_2(\mu) ,$$

where

$$P_1(\tau) = a_0 \exp(-a_0 \tau) , \tag{29}$$

$$P_2(\mu) = \frac{a_\mu}{a_0} . \tag{30}$$

The sum of all the probabilities $P_2(\mu)$ over all values of μ from 1 to n is equal to unity. Therefore, it is sufficient to obtain only one random number θ_1 for which $0 < \theta_1 < 1$ and find the range of $P_2(\mu)$ in the interval $[0, 1]$ where this number falls. The operation for finding μ is expressed as

$$\sum_{i=1}^{\mu-1} a_i < \theta_1 a_0 < \sum_{i=1}^{\mu} a_i , \tag{31}$$

i.e. we search for the value of μ satisfying inequalities (31). The time step τ is also specified by a single random number θ_2

as

$$\tau = \frac{1}{a_0} \ln \frac{1}{\theta_2} \tag{32}$$

in accordance with expression (29) for $P_1(\tau)$. When the time step τ and the μth reaction have been found, the current time t increases up to $t + \tau$ and the μth reaction is performed following stoichiometric relations. For one program cycle, only one of n reactions is conducted, which makes the calculation procedure time consuming. Nevertheless, the simulation method described above is correct and adequately represents the solution of the master equation [59] for one cell of volume V with good stirring.

The diffusion (or jump) of a particle from a cell into a neighbouring cell can also be responsible for a change in the number of particles in a cell, which can also occur with a certain probability [121]. The DSMC method, as described above, can hardly be used to treat numerous cells of CA, since the time step τ varies for each cell, and mass exchange cannot be performed simultaneously for two neighbouring cells at a moment t. When the value τ is equal for all the cells, the problem disappears. The authors of Ref. [122] proposed to determine τ as

$$\tau = \frac{1}{a_0} . \tag{33}$$

This relation is believed to be a good approximation for τ, since $1/a_0$ is the mean for random value (32). Note that only one reaction determined by Eqn (31) is performed during a cycle.

Another way to circumvent the above difficulties is to choose a small constant time interval Δt and to compare the probabilities of all the n reactions with n random numbers [123, 124]. In this case either all the n reactions or no reactions may take place during the interval Δt (depending on the random numbers sampled). On account of the difficulties in the choice of τ (or Δt) and the much time required for numerical calculations the DSMC method is not widely used to investigate spatially extended systems [43].

Since the DSMC method only deals with bimolecular reactions, the monomolecular and trimolecular ones cannot be modelled without any additional contrivances. For example, the monomolecular reactions of disappearance and appearance (feed rate) of molecules X, which are usually written as

$$X \rightarrow 0, \quad \rightarrow X , \tag{34}$$

in the case of the DSMC method take on the form

$$S + X \rightarrow S + S, \quad S + S \rightarrow X + S , \tag{35}$$
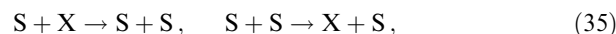
where S are the 'solvent' particles, whose concentration is constant. This constancy is attained by introducing some additional particles of species A which are not involved in any reactions but can change into the particles S and conversely so that the number of particles S in each cell does not change in the course of reaction (35).

The DSMC method is best suited for processes including only bimolecular reactions, where the typical time of all elementary reactions is the same, while the number of reactions is small. The DSMC method was successfully

applied to analyse thermal instabilities [107] and chemical oscillations [106, 114, 115].

6. The method of the probabilistic cellular automaton (PCA)

To solve the most complicated problems including the combined effects of reactions, diffusion, convection, and fluctuations, the method of the probabilistic cellular automaton with the use of the Monte Carlo procedure (PCA-MC or simply PCA) has been developed [33, 34]. The cellular automaton is a regular lattice consisting of $N^2 = N_0$ elementary cells (see Fig. 1). The lattice can be square as well as rectangular with a pronounced difference in side lengths. Each cell is characterised by a set of numbers such as the number of molecules of a relevant species in the cell (for example, n_X, n_Y, and n_Z when there are three sorts of molecules X, Y, and Z) and the coordinates (i and j) of the cell.

The cell has a volume V_m corresponding to the linear length $l = (V_m)^{1/3}$. The volume V_m is used to determine the probabilities of chemical reactions in cells. All the cells are assumed to be homogeneous, which imposes a limitation on the typical size and typical time:

$$l < l_{corr} = (D_0 \tau_{chem})^{1/2}, \qquad \tau_{diff} \equiv \frac{l^2}{D_0} < \tau_{chem}, \qquad (36)$$

where τ_{chem} is the time typical for a chemical reaction, while D_0 is the coefficient of molecular diffusion [125]. The cell size does not exceed the size of the smallest turbulent vortices. Hence, it should be less than the Kolmogorov size L_K defined as an inherent turbulent scale at which viscous forces play a great role [82]. Estimates show the cell size l to be less than $1 - 10\ \mu m$.

The PCA method is used to treat independently three processes such as molecular diffusion (the 'diffusion' procedure), chemical reactions (the 'chemistry' procedure), and turbulent stirring (the 'stirring' procedure). As a rule, periodic boundary conditions are used in these procedures, i.e., the cells of a lattice edge are proposed to be in contact with the cells of another edge.

6.1 The 'diffusion' procedure

The process of modelling diffusion by the PCA method is greatly sped up due to the abandonment of the one-step algorithm [81]. It is assumed in this paper that the mass exchange between neighbouring cells occurs as follows: the cells merge together for a short period when their contents mix totally, and then they decouple into two identical cells of the initial size. Such a dispersion-coalescence process takes place, for example, between water nanodroplets of reversed microemulsions [126, 127]. In this mechanism the probability $W(m, k|r, s)$ that two arbitrary neighbouring cells have m and k molecules of the same species at the moment $t + \text{StepDif}$, if they have r and s ($r + s = m + k$) molecules, respectively, at the moment t, is given by the binomial distribution

$$W(m, k|r, s) = \frac{(r+s)!}{k!\, m!}\, q^k (1-q)^m, \qquad (37)$$

where q is the ratio of the cell volume to the total volume of coalesced cells (in our case $q = 1/2$), and StepDif is a constant corresponding to a time step used to treat the diffusion process. Note that the constant is an actual time measured

in seconds. In the model the cell under consideration has eight neighbouring cells (see Fig. 1).

The numbers m and k are calculated as follows. Initially a pair of neighbouring cells is randomly chosen and the sum $r + s$ is calculated for it. Then a random value $\theta \in (0, 1)$ is generated and the number k satisfying the inequalities

$$\sum_{h=0}^{k} W(r + s - h, h|r, s) < \theta \leqslant \sum_{h=0}^{k+1} W(r + s - h, h|r, s) \quad (38)$$

is found under the condition $m = r + s - k$. A similar procedure is given by formula (31) in Section 5.

The intensity of mass exchange is controlled by the value of StepDif and the parameter ND determining the number $ND \times N_0$ of randomly chosen pairs of neighbouring cells during a time step StepDif. Mass exchange is performed independently for each species of molecules, corresponding to various numbers ND, for example, ND_X, ND_Y, and ND_Z for three species of molecules. As a rule, ND does not exceed 0.5. The ratio $ND/\text{StepDif}$ determines the frequency k_{ex} at which a particle jumps into an adjacent cell [33]:

$$k_{ex} = \frac{ND}{\text{StepDif}}. \qquad (39)$$

For a homogeneous water solution the quantities k_{ex} and V_m (or l) are related by the diffusion coefficient D_0:

$$D_0 \cong k_{ex} l^2. \qquad (40)$$

When there is not a direct relation between D_0, V_m and k_{ex} (for example, in the case of water droplets of the reverse microemulsion), the values V_m and k_{ex} are independent variables.

The validity of the considered mass exchange law has been tested in various problems of mathematical physics. For instance it is well known that in the one-dimensional case the dynamics of smoothing of a sharp interface between two initially uniform regions with different concentrations of a substance follows the law [128]:

$$\frac{\partial c}{\partial x} = \frac{c_0}{2(\pi D_0 t)^{1/2}} \exp\left(-\frac{x^2}{4 D_0 t}\right). \qquad (41)$$

Assuming for the two-dimensional case that $c(x) = \langle n_{Z,i} \rangle$, where $\langle n_{Z,i} \rangle$ is the number of particles Z averaged over the cells of the ith column, the column number i corresponds to the coordinate x, and believing the initial numbers of particles $n_{Z,i}$ in the left and right parts of the lattice to be equal to n_1 and n_2 respectively (for instance, $n_1 = 100$ and $n_2 = 0$), the author found by the PCA method [33] that the change in $\langle n_{Z,i} \rangle$ is exactly the same with the law (41). The mean square displacement $\langle r^2 \rangle$ of particles was shown to be proportional to the coefficient D_0 of molecular diffusion and time t, i.e., $\langle r^2 \rangle \propto D_0 t$. The evidence for the applicability of the diffusion law used [formulas (37) and (39)] is the fact that any initial distribution of particles over cells tends in the limit $t \to \infty$ to the Poissonian one (in the absence of chemical reactions).

6.2 The 'stirring' procedure

The main concepts used to model turbulence by the PCA method are based on the idea described in Section 2, i.e. a hierarchy of scales for turbulent motion, however with modified frequency of running the procedure and sizes of

chosen squares. The procedure is carried out in constant time intervals StepMix, the time interval StepMix as well as StepDif being measured in seconds. The size L $(L < N)$ of a square chosen in an arbitrary place on the lattice is a random value available for the procedure. The intensity of stirring is controlled by the time interval StepMix and the smallest size of the chosen squares.

Combined operation of the 'stirring' and 'diffusion' procedures allows one to find the rate constant k_{mix} for stirring. It can be obtained numerically in measurements of stirring of two equal parts of a lattice, whose cell states are initially different (as in the numerical experiments on testing the 'diffusion' procedure). The coefficient k_{mix} can be found by calculations of the time dependence of $\sigma^2 - \sigma_{eq}^2$ and with the use of the approximation for the difference $\sigma^2 - \sigma_{eq}^2$

$$(\sigma_0^2 - \sigma_{eq}^2) \exp(-k_{mix}t), \qquad (42)$$

where σ^2 is the dispersion determined by Eqns (15) and (16), σ_0^2 is the dispersion at the moment $t = 0$, and σ_{eq}^2 is the equilibrium dispersion in the limit $t \to \infty$, $\sigma_{eq}^2 = \langle n \rangle$. In the semilogarithmic coordinates $t, \ln(\sigma^2 - \sigma_{eq}^2)$ the dependence of $\sigma^2 - \sigma_{eq}^2$ on time t is virtually a straight line.

The rate constant k_{mix} depends on the micromixing determined by the constant k_{ex} of microstirring as well as on the rate of macrostirring. When the rate of turbulent stirring is rather high (the time interval StepMix is short) the rate constant k_{mix} is controlled by diffusion so that $k_{mix} \cong k_{ex}$. As StepMix and the spatial scale of turbulence rise, macrostirring determined by the 'stirring' procedure may become the limiting stage of the process of stirring.

6.3 The 'chemistry' procedure

For any chemical reaction there is a probability that the number of particles involved in it may change during the interval τ in the volume V_m. For a monomolecular reaction of disappearance of particles X, occurring in the volume V_m containing $n = n_X = [X]V_m N_A$ particles X and having the rate constant γ, the probability $p(k|n)$ for k particles of species X to disappear during the interval τ is given by the binomial distribution

$$p(k, n) = C_n^k \chi^k (1 - \chi)^{n-k}, \qquad (43)$$

where $C_n^k = n!/(k!(n-k)!)$, $k = 0, 1, \ldots, n$; $\chi = \gamma\tau$, $0 < \chi < 1$. To simplify calculations, the PCA method only deals with one-step processes, for which $k = 1$ and the time interval τ is calculated so that the following inequality is fulfilled for all γ and n $(n \neq 0)$:

$$n\gamma\tau < 0.1. \qquad (44)$$

In this case, distribution (43) yields $p(1|n) \cong n\gamma\tau$.

Reasoning in a similar way, we can find the probabilities for reactions of any type. Table 1 lists the probabilities W_i for various reactions to occur in the volume V_m during the period τ. In computer simulations of the ith chemical reaction a random number θ $(\theta \in [0, 1])$ is generated at each time step τ for each cell. If the inequality $\theta < W_i$ is fulfilled for a cell, the ith reaction is realised in the cell. The time step τ is calculated for each discrete moment so that the relation

$$\max\{W_i\} = 0.1 \qquad (45)$$

takes place on condition that the maximum $\max\{\ \}$ is calculated for all cells at each time step τ, while the values of

Table 1. Probabilities W_i of various reactions, found by the PCA method.

Reaction	Simulation	γ_i, s^{-1} [1]	W_i
$\to X$	$n_X \to n_X + 1$	$C_0 V_m N_A$ [2]	$C_0 V_m N_A \tau$
$X \to 0$	$n_X \to n_X - 1$	k	$k n_X \tau$
$A + X \to 2X$	$n_X \to n_X + 1$	$k\,[A]$ [3]	$k[A] n_X \tau$
$X + Y \to Z$	$n_X \to n_X - 1$ $n_Y \to n_Y - 1$ $n_Z \to n_Z + 1$	$\dfrac{k}{V_m N_A}$	$\dfrac{k}{V_m N_A} n_X n_Y \tau$
$X + X \to 0$	$n_X \to n_X - 2$	$\dfrac{k}{V_m N_A}$	$\dfrac{k}{V_m N_A} n_X (n_X - 1)\tau$
$3X \to 2X + Y$	$n_X \to n_X - 1$ $n_Y \to n_Y + 1$	$\dfrac{k}{(V_m N_A)^2}$	$\dfrac{k}{(V_m N_A)^2} n_X(n_X-1)(n_X-2)\tau$

[1] The constants γ_i of the quasi-first order determine the rates of the corresponding reactions.
[2] The rate of increase C_0 in the number of particles X is measured in M s^{-1}.
[3] The number of particles A is assumed to be huge and does not change during the reaction.

variables n_X, n_Y, and others, if any, are taken from the previous moment $t - \tau$. With this definition of τ inequality (44) is fulfilled. The interval τ depends on the stage of the reaction and can vary over several orders of magnitude. As the number of particles in a cell increases in the course of the reaction, the interval τ increases and vice versa.

Let us consider more fully the case when the number of particles in a cell is small (does not exceed the sum of stoichiometric coefficients for reactions involving the particle under study). Let us assume that there are two reactions resulting in a decrease in the number n_X of particles in a cell, for instance, (22) and (25), and that at a moment t for a certain particle $n_X = 2$ and $n_Y \geqslant 1$. If at moment $t + \tau$ two random numbers are generated, which are respectively less than W_{22} and W_{25}, both the reactions have to take place. However, if reaction (22) [or (25)] is the first to occur, the number n_X is equal to unity (zero) and the other reaction cannot proceed. If the sequence of reaction occurrence is determined by the program, for example, reaction (22) proceeds before reaction (25), then the actual probability for reaction (25) to occur is less than $W_{25} = n_X(n_X - 1)k_2\tau/2$. To minimise this error, we used the following expedient. The reactions which resulted in the increase in the number of particles (if any) were assumed to proceed first. Two versions of the order of proceeding reactions (22) and (25) were randomly altered. If the versions were more they randomly altered with equal probability of occurrence. As a result, under the conditions $n_X = 2$, $n_Y \geqslant 1$ the actual probabilities w_{22} and w_{25} of reactions (22) and (25) to take place are given by

$$w_{22} = W_{22}\left[1 - \frac{W_{25}(1 - W_1)}{2}\right],$$

$$w_{25} = W_{25}\left[1 - \frac{W_{22}(1 - W_1)}{2}\right], \qquad (46)$$

where W_1 is the probability of occurrence of a reaction (or a sum of reactions) increasing the number of particles X. Since $W_i < 0.1$, the probabilities w_{22} and w_{25} differ from W_{22} and W_{25} respectively by no more than 5%. In view of the fact that the conditions $n_X = 2$ and $n_Y \geqslant 1$ are not fulfilled for many cells, this difference is still less. In the case of a Poissonian

Table 2. Main parameters and characteristics of the 'diffusion', 'stirring', and 'chemistry' processes modelled by the PCA method[1].

Parameters	Molecular diffusion	Turbulent stirring	Chemical reactions
Time step between running the procedure	StepDif	StepMix	τ
The number of operations in the procedure	$ND \times N_0$	$\sum_{L=1}^{\text{Lev}} N_L$	nN_0
Probability of execution of single operations	$W(m, k\vert r, s)$	W_s	W_i
The pseudo-first order constants characterising the rate of the process	k_{ex}	k_{mix}	γ_i

[1] The probabilities W_i and constants γ_i are given in Table 1. N_0 is the number of elementary cells in the square lattice of the CA; n is the number of considered chemical reactions, i is the index of the chemical reaction; W_s is the probability that at least two out of four quadrants of a randomly chosen square $L \times L$ will be interchanged during an operation; $W_s = 3/4$; N_L is the number of samples of a square of size L; the variable Lev determines the smallest size of considered squares (turbulent scale).

distribution of particles X and Y, the differences of w_{22} and w_{25} from W_{22} and W_{25} do not exceed 1%, and are usually less than 0.1%. The difference is immaterial for a system which does not have any critical points or is shifted by 1% from a critical point.

Table 2 presents the main parameters and rate constants for all the three processes modelled by the PCA method. The validity of the method was checked by comparing the numerical results with the exact analytical solutions to the simplest equations as well as with the numerical solution to a complicated set of ODE. The difference is negligible except for small fluctuations at small numbers n_X and n_Y.

7. Potential of LGCA, DSMC, and PCA methods in examining the Willamowski – Rössler model

7.1 Advantages and limitations of the LGCA, DSMC, and PCA methods

To start with we outline the main advantages, peculiarities, and limitations of the LGCA, DSMC, and PCA methods described in Sections 4 – 6. All the methods treat chemical reactions at a mesoscopic level which deals with scales larger than the scales used in molecular dynamics and smaller than those used in the CA-ODE and other related models. The variables of all the methods are discrete numbers equal to the number of particles of a certain species in small spatial regions (cells). The LGCA, DSMC, and PCA methods take into account in a natural way the influence of internal fluctuations on the macroscopic behaviour of the system. In all the methods the cells are considered to be homogeneous, i.e. the probability for two particles residing in a cell to collide is the same for all the particles, in other words, all the particles in the cell have the same spatial coordinates. The DSMC method yields results similar to the solution of the master equation, and, in a sense, is a unique test to check this equation [43]. The same is probably true for the LGCA and PCA methods, however a direct comparison with the master equation has not been performed for these methods.

The DSMC and PCA methods preset the probabilities for elementary chemical reactions to occur, while the LGCA method specifies the probabilities for the number of particles in a cell to change, the latter being a sum of the probabilities of the occurrence of all chemical reactions involving these particles. Therefore it is not necessary to determine a sequence of reactions for the method.

The DSMC and LGCA methods, in a sense, trace their origin to gas-dynamics ideas, such as a Boltzmann gas
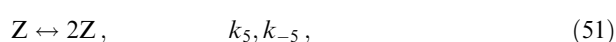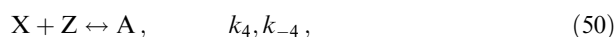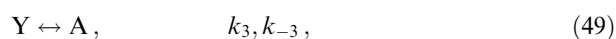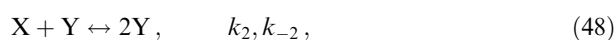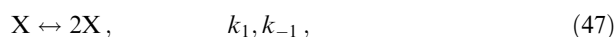
(particles treated as hard spheres), for which the notions of the length of free flight motion and velocity of a particle are applicable. In DSMC and LGCA methods these notions are extended to diffusion in liquids, where, however, they have no physical meaning. The PCA method does without these notions, but uses the idea of fusion – fission of liquid droplets or neighbouring cells (nanovolumes).

The DSMC method only applies for bimolecular reactions. To treat monomolecular and trimolecular reactions some artificial expedients are required. The LGCA and PCA methods do not have this disadvantage. The DSMC method yields correct results when typical times of elementary reactions are rather close and the number of species of particles is small. As for LGCA and PCA methods, a pronounced difference in the typical times of reactions and a large number of species increase the time of calculations but do not impair the results.

The DSMC method is mainly used to investigate the influence of fluctuations on homogeneous dynamical systems and in a few works — to consider the reaction – diffusion equations, however, only in the one-dimensional case. The LGCA method is chiefly applied to spatially extended systems, i.e. reaction – diffusion equations. The PCA method is used both to describe point systems with regard to fluctuations as is the DSMC method, and to treat spatially extended systems as is the LGCA method. There are not any restrictions on the use of the methods in the three-dimensional case. But only the PCA method can treat reaction – diffusion – convection problems at present. The DSMC and LGCA methods are only applied to reaction – diffusion equations.

7.2 The Willamowski – Rössler model

Unfortunately the LGCA, DSMC and PCA methods have not been used to investigate the same problem under identical conditions, therefore, a direct comparison is rather difficult. The most suitable model to demonstrate the potential and validity of all the methods is the Willamowski – Rössler (WR) model presented by the following set of reactions [129, 130]

$$X \leftrightarrow 2X, \qquad k_1, k_{-1}, \qquad (47)$$

$$X + Y \leftrightarrow 2Y, \qquad k_2, k_{-2}, \qquad (48)$$

$$Y \leftrightarrow A, \qquad k_3, k_{-3}, \qquad (49)$$

$$X + Z \leftrightarrow A, \qquad k_4, k_{-4}, \qquad (50)$$

$$Z \leftrightarrow 2Z, \qquad k_5, k_{-5}, \qquad (51)$$

where the subscripts + and − of the rate constants k denote direct and inverse reactions respectively.

The WR model was studied by the LGCA [24, 35], DSMC [114], and PCA methods. Structurally, the WR model is a combination of two models: (1) the well-known Lotki – Volterra model [reactions (47) – (49)], where the particles X and Y related by reaction (48) increase in number autocatalytically and (2) the 'switch' model [reactions (47), (50), and (51)] where the particles of Z species can also multiply. The Lotki – Volterra model yields structurally unstable oscillations, while the 'switch' model has two stable states [the concentration of Z is high, while the concentration of X is small (about zero), and vice versa]. The combination of these two models gives rise to a multiplicity of dynamic regimes including direct and inverse cascades of period doubling bifurcations routing to chaotic oscillations in a homogeneous well stirred system, autowave phenomena and Turing structures in a spatially extended system without stirring. Figure 4 plots the phase diagrams of various dynamic regimes of a point (0D) WR model for varied constant k_{-1} (the constant k_{-1} has the dimension M^{-1} s^{-1} which will be omitted in what follows). Fig. 5 depicts the bifurcation diagram for the WR model. As is seen from the figure, in the range of constant k_{-1} values from 0.41 to 0.6 the model exhibits chaotic oscillations.

The influence of fluctuations as the WR system transits through bifurcation points and occurs nearby or inside the region of chaotic oscillations was investigated by the LGCA
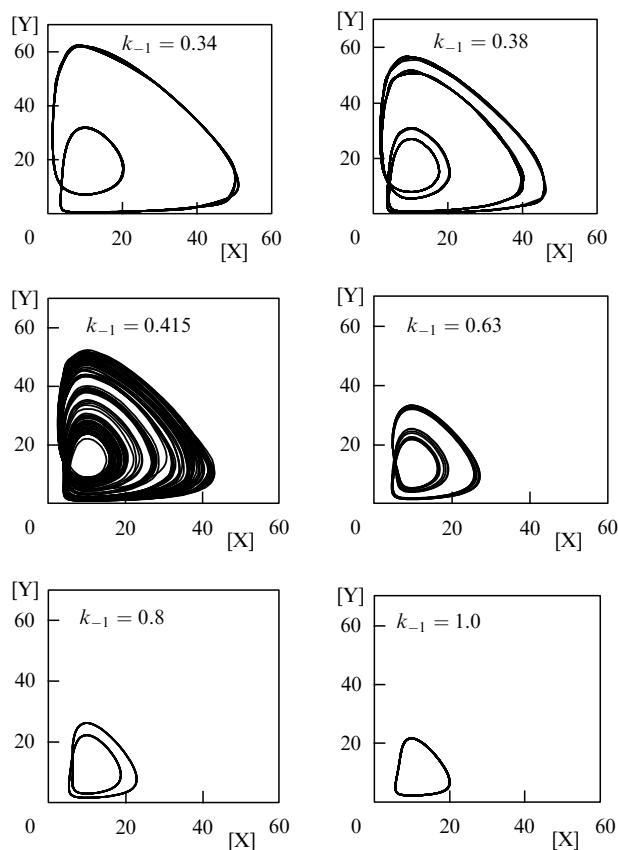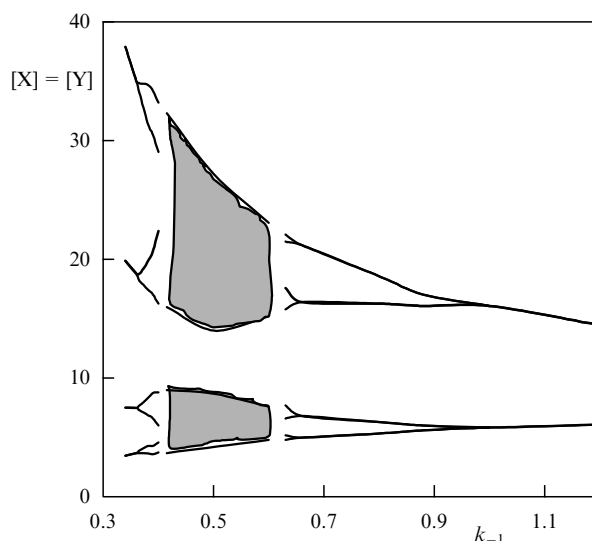

Figure 5. Bifurcation diagram of the point Willamowski – Rössler model (47) – (51) obtained by integration of a set of ODE. Plotted on the vertical axis are the X values of intersections of the attractor by the plane [X] = [Y]. The values of the other constants are the same as in Fig. 4.

[24, 35] and the PCA methods. The study by the LGCA method was carried out for two limiting cases, i.e. for a spatially distributed system without stirring and for a point system with strong stirring. The PCA method was used to investigate intermediate cases as well. It is obvious that the influence of fluctuations on the system must increase as the controlling parameter (for example, constants k_{-1} or k_2) tends to the region corresponding to chaotic oscillations. In the deterministic system without fluctuations the values of bifurcation points are determined exactly and show well on the bifurcation diagram (Fig. 5), while with the availability of fluctuations the bifurcation transitions become rather diffused. This results from the diffusive spreading of the orbits of periodical motion, and spreading and merging of the bands of the chaotic attractor. The fluctuactive limiting cycle and the chaotic attractor become hardly distinguishable (see, for example, Fig. 6 showing the limiting cycle and chaotic attractor found by the PCA method at $k_{-1} = 0.34$ and $k_{-1} = 0.415$ respectively).

However, in the case of the limiting cycle ($k_{-1} = 0.34$) the attractor with large fluctuations can be transformed into one relatively close to a well-determined periodical orbit. One way to do this is to increase the cell volume V_m, and hence, the number of particles in the cell. Alternatively, one can magnify the diffusion coefficient and enhance the intensity of stirring. These procedures do not change noticeably the shape of the strange attractor, as is seen from Fig. 7 which shows the same attractors as in Fig. 6 but at large value k_{ex} and small value StepMix.

The influence of internal fluctuations on deterministic chaos is also clearly seen from the comparison of Poincare cross-sections found by numerical solution of the relevant ODE and those obtained by the PCA method, as well as from comparison of corresponding next amplitude maps constructed from the Poincare cross-sections. Figure 8 plots sections of the strange attractor (obtained by numerical integration of ODE) intersected by the plane [X] = [Y] (a) and its next amplitude map $[Z]_{n+1} = f([Z]_n)$ (b), where $[Z]_n$ is the Z-coordinate of the Poincare cross-section at the moment

Figure 4. Projections of three-dimensional attractors of the point Willamowski – Rössler model (47) – (51) on the plane X – Y (X, Y, and Z are expressed in mole/litre) for various constants k_{-1}. $k_1 = 30$ s^{-1}; $k_2 = k_4 = 1$ M^{-1} s^{-1}; $k_3 = 10$ s^{-1}; $k_{-2} = k_{-3} = k_{-4} = 0$; $k_5 = 16.5$ s^{-1}; $k_{-5} = 0.5$ M^{-1} s^{-1}.
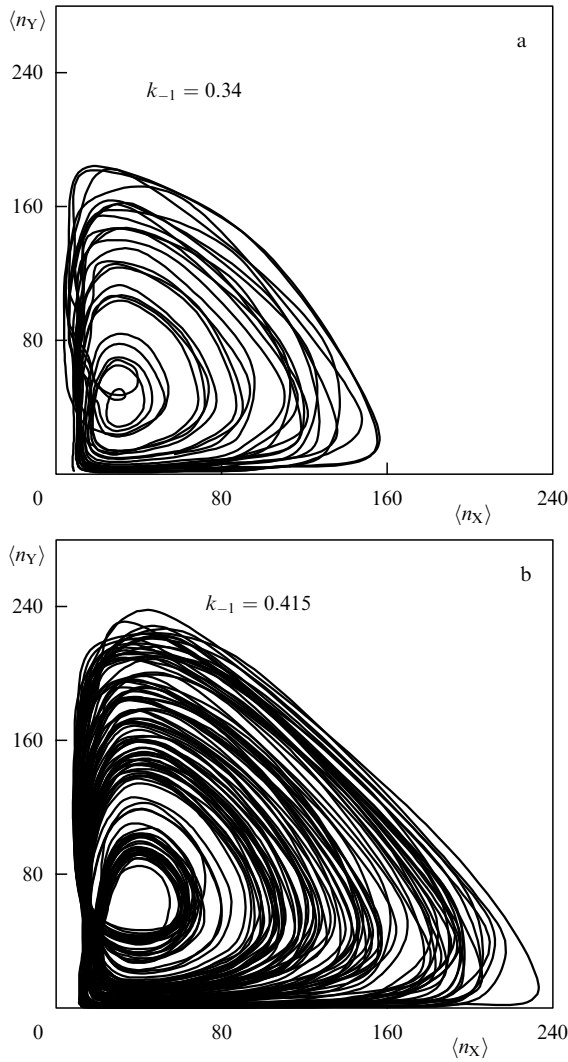
Figure 6. Limiting cycle and strange attractor found by the PCA method in the WR model at $k_{-1} = 0.34$ (a) and $k_{-1} = 0.415$ (b), the other constants are the same as in Fig. 4. The CA parameters are $N \times N = 48 \times 48$, $V_m N_A = 3$ M^{-1}, $k_{ex} = 500$ s^{-1}, Lev = 4, StepMix = 0.1 c in case (a) and $N \times N = 16 \times 16$, $V_m N_A = 4$ M^{-1}, $k_{ex} = 1000$ s^{-1}, Lev = 3, StepMix = 0.01 s in case (b).
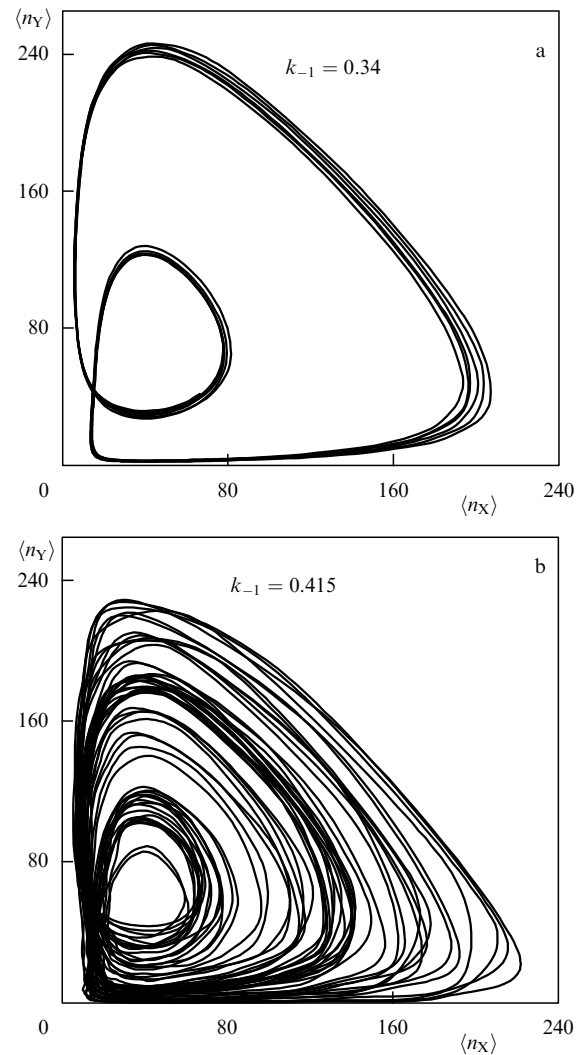
Figure 7. Limiting cycle and strange attractor found by the PCA method in the WR model at $k_{-1} = 0.34$ (a) and $k_{-1} = 0.415$ (b). All the CA parameters are the same as in Fig. 6, except for $k_{ex} = 1000$ s^{-1}, StepMix = 0.01 s in case (a) and $k_{ex} = 5000$ s^{-1}, StepMix = 0.001 s in case (b).

t_n, while $[Z]_{n+1}$ is the Z-coordinate at the next moment t_{n+1}. Figure 8c, d depict similar dependencies for the same attractor at $k_{-1} = 0.415$, found by the PCA method. As is seen, the shape of curve $Z_{n+1} = f(Z_n)$ typical for chaotic oscillations is not affected by internal fluctuations in the WR model. However the scatter becomes larger in the fluctuactive system.

The WR system in an oscillatory or chaotic state may generate time-dependent unstable spatial structures when stirring is lacking and the diffusion is not strong enough to homogenise the whole system. This phenomenon is referred to as *spatio-temporal turbulence*. The attractor of the system decreases in the phase space, while the dispersion greatly exceeds the equilibrium Poisson value. Figure 9 plots the images (maps) for Z particles found by the PCA method in simulating the WR model in the regime of chaotic oscillations at the moments t_1 and t_2. Black, grey, and white regions are discernible in the figure corresponding to different densities of Z particles. These regions evolve in time. Spatial structures arise [35] when the inequality $l_{corr} < lN$ is fulfilled, where l_{corr} is determined by (36), l is the cell size, while lN is the lattice

size. The occurrence of spatial structures similar to nuclei makes one to calculate the effect of fluctuations not for the whole system, but for a small region of correlated size l_{corr}. In such regions fluctuations are great and can change the behaviour of the system.

When the system is intensively stirred the amplitude of fluctuations can depend on the size of the whole system. The larger the value $N \times N$, the smaller the fluctuation effect, all the other factors being equal. It was shown [35] that there exists a critical size of the system above which the difference between fluctuactive and deterministic attractors is small (see, for example, Fig. 7a and 4a). As the size of the system decreases fluctuations can change the limiting cycle to a state differing only slightly from the strange attractor (see Fig. 6a, 4a, and 4c). The effect is similar to transitions induced by external noise [131].

All the foregoing fluctuation effects were obtained by the LGCA and PCA methods. The WR model was studied at various diffusion coefficients only by the PCA method. Varying the ratio between the diffusion coefficients D_X, D_Y, and D_Z (or jump constants k_X, k_Y, and k_Z) it was revealed that
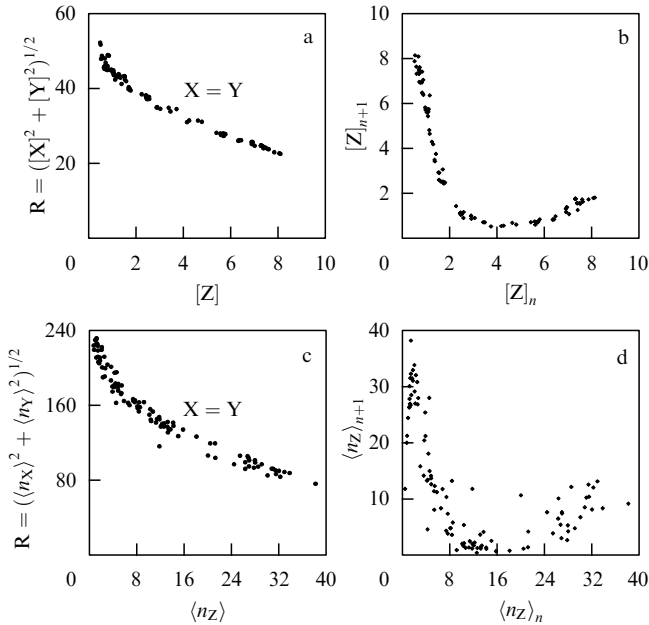
Figure 8. Poincare cross-sections (a, d) for a strange three-dimensional attractor in the WR model and their one-dimensional next amplitude maps found by numerical calculation of ODE (a, b) and by the PCA method (c, d) at $k_{-1} = 0.415$. The other constants are the same as in Fig. 4. The parameters of the PCA model are the following $N \times N = 16 \times 16$, $V_m N_A = 4$ M^{-1}, $k_{ex} = 1000$ s^{-1}, Lev = 3, StepMix = 0.01 s (as in Fig. 6b).

Figure 9. Images of the Z map at moments $t_1 = 1.2458$ s (a) and $t_2 = 1.7152$ s (b) found in the WR model by the PCA method at $k_{-1} = 0.415$. The other constants are the same as in Fig. 4. The lattice parameters are the following $N \times N = 48 \times 48$, $V_m N_A = 4$ M^{-1}, and $k_{ex} = 10$ s^{-1}.

stationary structures (Turing structures) may arise in an initially homogeneous system without stirring on the condition

$$k_X \ll k_Y, \qquad k_Z \ll k_Y. \tag{52}$$

We emphasise that the term 'Turing structures' refers to the structures arising in the system, whose point (0D) equations have a stationary state. The above example is probably the first case when the formation of stationary structures does not depend on the state of the dynamical system, which can be in the oscillating, chaotic, or stationary states. Figure 10 plots changes in the Turing structures as the constant k_{-1} varies over the range corresponding to different dynamic regimes of the point WR model. It is seen that, as k_{-1} rises, the typical size of the structures increases. The structures are rather stable with respect to fluctuations whose amplitude is changed by varying the cell volume V_m.
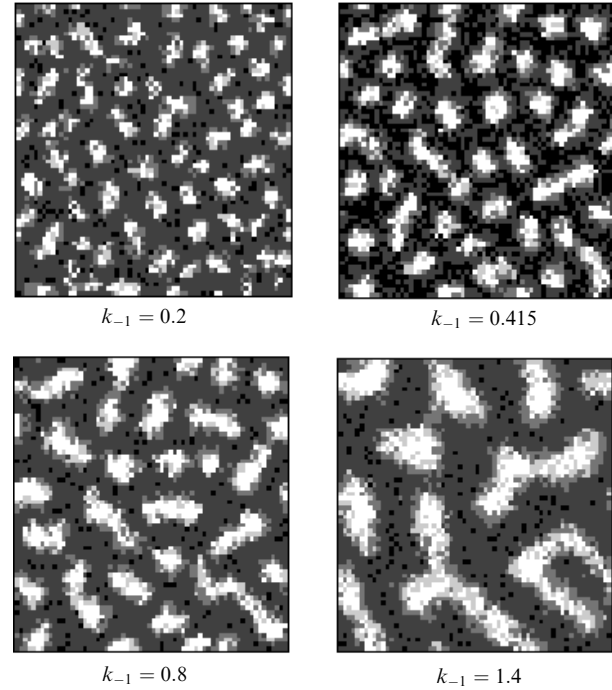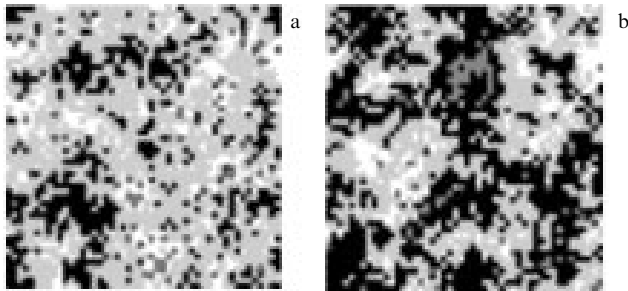

Figure 10. Stationary (Turing) structures consisting of Z particles obtained by the PCA method for the WR model. Increased darkness corresponds to an increased concentration of particles. The lattice parameters are: $N \times N = 64 \times 64$; $V_m N_A = 1$ M^{-1}; $k_X = k_Z = 5$ s^{-1}; $k_Y = 500$ s^{-1}. The constants are the same as in Fig. 4.

The effect of fluctuations on the propagation of auto-waves in oscillating and chaotic media was studied by the LGCA method [24]. It was shown that fluctuations may give rise to additional waves, whose existence does not follow from the solution to the corresponding deterministic reaction–diffusion equations.

To conclude the section we outline briefly the results of the analysis [114] of a homogeneous WR model by the DSMC method. Paper [114] compares the probability density functions and power spectrum of the strange attractor found by the DSMC method with those obtained by numerical solution of the master equation. The data obtained by both the methods were shown to be in good agreement. This conclusion was confirmed in studies of a simpler system [15, 43, 108] which testifies to the reliability of the results obtained by the solution of the master equation. Note also that in these works an important theoretical result was obtained by the DSMC method. Namely, it was found that the Langevin and master equations yield the same results only for systems with one stable state. In bistable systems the bimodal functions of probability density, derived from the solution of these equations, are different. The DSMC method yields the function of the probability density, coinciding with that found from the master equation. This suggests that the Langevin equation cannot be used to study multistable systems. Note that the PCA method yields the same data as the DSMC method (unpublished data).

8. Examples of some problems solved by the PCA method

In the previous section we dealt with various effects of fluctuations on a hypothetical WR model. Here we will

consider actual chemical systems and the ways to treat them by the PCA method.

### 8.1 Reactions of X + Y → 0 and X + X → 0 types

The influence of diffusion, fluctuations, and dimensionality of space on reactions of the type of (22) and (25) has been considered in many papers [83, 95, 132–142], and now the dynamics of these reactions is thoroughly studied. It is well known [133] that the reaction $X + Y \rightarrow 0$, whose rate constant k_{diff} is controlled by diffusion demonstrates a clustering effect which is as follows. The particles of species X and Y initially randomly distributed in space with the same averaged concentrations rearrange with time so that clusters of particles arise, where particles of one species are present, while particles of the other one are lacking. The reaction takes place at the cluster boundary. As a result, the observed rate constant decreases, and the reaction deviates from the classical law

$$[X]^{-1} - [X]_0^{-1} = k_{diff}t, \qquad (53)$$

in particular, the asymptotic time-dependence of [X] changes.

These results were obtained both analytically and with the help of lattice models used in the Monte Carlo method. In most lattice models the rate constant of the chemical reaction is assumed to be equal to infinity. This means that if there are two particles X and Y in a cell, they annihilate in a moment. In this case the reaction rate is completely determined by the rate of random wandering over the lattice, i.e. diffusion. In the PCA method the rate k_{chem} of a chemical reaction is assumed to be finite. But if the rate k_{chem} exceeds greatly the rate k_{ex} of jumps, the reaction is controlled by diffusion. Figure 11 plots the lattice maps for particles X and Y obtained by the PCA method after a great lapse of time from the onset of the reaction (22). We can see clusters occupied by particles of species X (particles in the left side of the lattice) and Y (particles in the right side of the lattice). In the reaction $X + X \rightarrow 0$ controlled by diffusion the fluctuations also decrease the rate constant of a reaction occurring in a space, whose dimensionality d is less than the critical one d_c [137, 143, 144].

The PCA method allows one to represent adequately the transition from the regime controlled by chemical reactions to that controlled by diffusion. As an example we consider the reaction [50]

$$X + X \rightarrow X + A, \qquad k_{2-1}, \qquad (54)$$
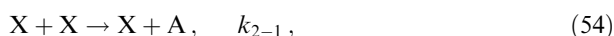
whose rate is written as

$$\frac{dn_X}{dt} = -k'_{2-1}n_X^2. \qquad (55)$$

It follows that

$$\frac{1}{n_X} - \frac{1}{n_0} = k'_{2-1}t, $$

where $k'_{2-1} = k_{2-1}/(V_m N_A)$. The kinetic curves $\langle n_X \rangle = f(t)$ for reaction (54) were obtained on a lattice of size 128×128 at various diffusion constants k_{ex} for the initial Poissonian distribution of particles with the mean value $n_0 = 0.25$ on condition of strong stirring. For all the studied cases the kinetic curves appear as straight lines in the coordinates
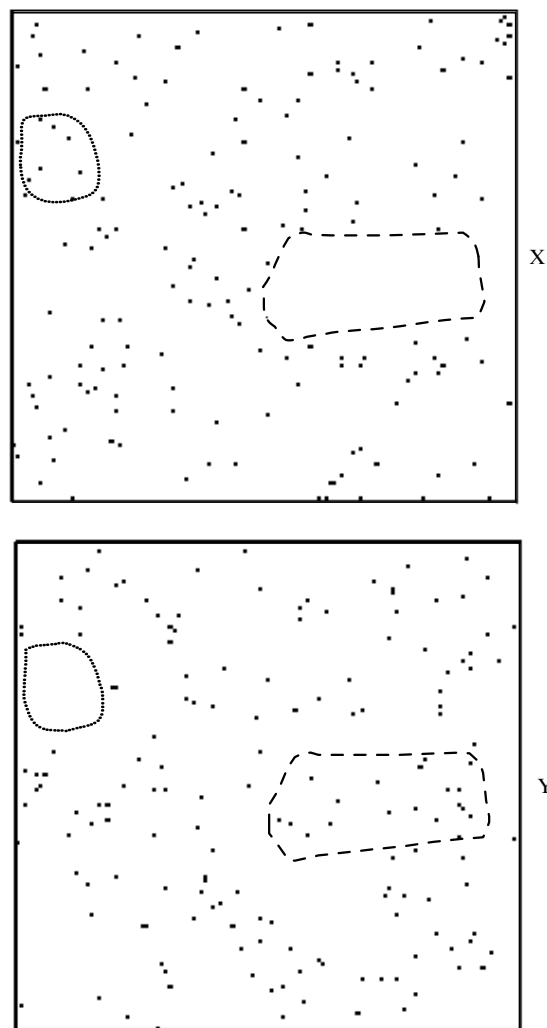

Figure 11. X and Y lattice maps obtained by the PCA method for the reaction $X + Y \rightarrow 0$. The initial distribution of particles over cells is binomial, the initial averaged number of particles in the cells is $\langle n_X \rangle_0 = \langle n_Y \rangle_0 = 1$. The maps correspond to a density of particles equal to $\langle n_X \rangle = \langle n_Y \rangle = 0.01$ and constants $k_1 = 10^9$ M^{-1} s^{-1}; $k_1/(V_m N_A) = 10^3$ s^{-1}; $k_{ex} = 50$ s^{-1}; $N \times N = 256 \times 256$. Each pixel on the map represents a cell with a single particle of X or Y species.

$(1/\langle n_X \rangle - 1/n_0, t)$. The effective constant $(k'_{2-1})_{eff}$ was determined as the slope of the lines. Note that the effective constant $(k'_{2-1})_{eff}$ is independent of the shape of the initial distribution and the value $\langle n_X \rangle_0$ when this value is less than unity. Figure 12 plots the dependence of $(k'_{2-1})_{eff}$ on k_{ex}, which is described by the equation

$$(k'_{2-1})_{eff} = \frac{\gamma k_{ex} k'_{2-1}}{\gamma k_{ex} + k'_{2-1}}, \qquad (56)$$

where $\gamma = 0.463$. As follows from (56) if $\gamma k_{ex} \ll k'_{2-1}$ then $(k'_{2-1})_{eff} = \gamma k_{ex}$, i.e. the effective rate constant is completely determined by the diffusion coefficient.

8.2 Luminescence quenching in micelles (X + Y → Y)

A particular and important case of reactive interaction between two particles is the reaction
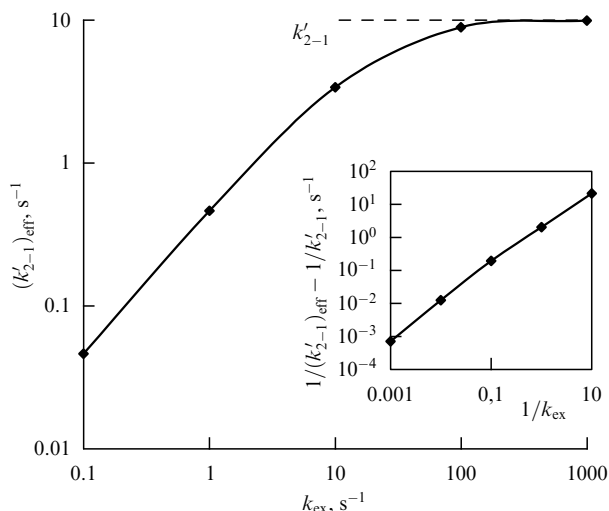
$$X + Y \rightarrow Y + A, \qquad k_3, \qquad (57)$$

Figure 12. Dependence of $(k'_{2-1})_{eff}$ on k_{ex} obtained by the PCA method for reaction (54). The inset shows the same dependence on the plane $(1/k_{ex}, 1/(k'_{2-1})_{eff} - 1/k'_{2-1})$. The constants are the following $k_{2-1} = 10^8 \text{ M}^{-1} \text{ s}^{-1}$, $k'_{2-1} = k_{2-1}/(V_m N_A) = 10 \text{ s}^{-1}$, $\langle n_X \rangle_0 = \langle n_Y \rangle_0 = 0.25$ [50].

Figure 13. Kinetic curves for the reaction $X + Y \rightarrow Y$. The dashed curves correspond to the solution of the Infelta – Tachiya equation, while the solid ones are obtained by the PCA method under initial conditions $n_X = 1$ and $\langle n_Y \rangle = 4$ (a Poissonian distribution of particles Y over cells). The parameters used for the Infelta – Tachiya equation are the following $\langle n_Y \rangle = 4$, $k_r = 10 \text{ s}^{-1}$, and $k_{ex} = 0$ (curve *1*), $k_{ex} = 1 \text{ s}^{-1}$ (curve *2*), $k_{ex} = 9.8 \text{ s}^{-1}$ (curve *3*), $k_{ex} = 45 \text{ s}^{-1}$ (curve *4*), and $k_{ex} = 135 \text{ s}^{-1}$ (curve *5*), while the parameters used for the PCA method are $k_3 = 10^6 \text{ M}^{-1} \text{ s}^{-1}$, $V_m N_A = 10^5 \text{ M}^{-1}$, $k_3/(V_m N_A) = k_r = 10 \text{ s}^{-1}$, StepDif $= 10^{-3}$ s, $k_{ex, X} = 0$ (X molecules are not diffused), $k_{ex, Y} = 0$ (curve *1*), $k_{ex, Y} = 1 \text{ s}^{-1}$ (curve *2*), $k_{ex, Y} = 10 \text{ s}^{-1}$ (curve *3*), $k_{ex, Y} = 50 \text{ s}^{-1}$ (curve *4*), and $k_{ex, Y} = 10^3 \text{ s}^{-1}$ (curve *5*); $N_0 = 64^2$ [33].

which describes luminescence quenching in solution and micelles, X is a luminescent particle in a photoexcited state (probe), Y is the quenching molecule or ion (quencher), while A is the luminescent particle in the ground state. The exact time-dependence of $\langle n_X \rangle$ is determined by the well known Infelta – Tachiya equation [145, 146]

$$\langle n_X(t) \rangle = \langle n_X \rangle_0 \exp \left\{ - \frac{\langle n_Y \rangle k_{ex} k_r}{k_{ex} + k_r} t \right.$$
$$\left. - \frac{\langle n_Y \rangle k_r^2}{(k_{ex} + k_r)^2} \left[1 - \exp \left(-(k_{ex} + k_r) t \right) \right] \right\}, \quad (58)$$

where $\langle n_X \rangle$ is the number of X particles, averaged over the microvolume V_m, which will be taken to mean the water core of nanodroplets of reverse microemulsion, $k_r = k_3/(V_m N_A)$; k_{ex} is the quasi-first order rate constant of mass exchange between microvolumes, $k_{ex} = k_e C_m$; k_e is the bimolecular rate constant of mass exchange, C_m is the concentration of microvolumes (nanodroplets) in the whole system [in the PCA method it is given by Eqn (39)]. This complicated form of Eqn (58) results from the Poissonian distribution of quencher particles over nanodroplets.

Figure 13 plots the kinetic curves obtained by the PCA method and by analytical solution of Eqn (58). It is seen that the curves obtained by the two methods are in agreement, the slight difference in the results has a statistical character and varies from experiment to experiment. When $k_{ex} \gg k_r$, Eqn (58) takes the conventional form

$$\langle n_X(t) \rangle = \langle n_X \rangle_0 \exp \left(-\langle n_Y \rangle k_r t \right). \quad (59)$$

In this case the time dependence of $\langle n_X \rangle$ is a straight line in the semilogarithmic scale $(\ln \langle n_X \rangle, t)$ (see, curve *5* in Fig. 13). When $k_{ex} \ll k_r$, i.e. reaction (57) is limited by diffusion, the fluctuation effect becomes noticeable and the kinetic curves (curves *1* and *2*) differ significantly from curve *5*. Reaction (57) was studied in Ref. [147] on one-, two-, and three-dimensional lattices.

Equation (58) is widely used to find the rate constant k_{ex} of mass exchange between nanodroplets in interpreting
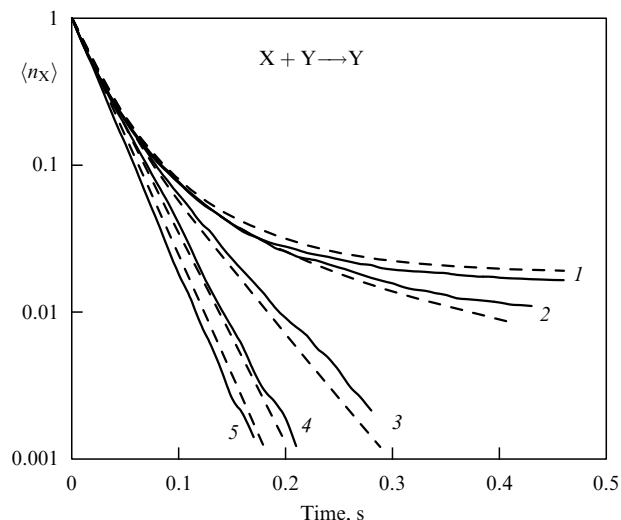
kinetic curves obtained in experiments on dynamic (or time-resolved) quenching of luminescence where a luminescent particle A is photoexcited by a pulse [148 – 150]. The PCA method allows one to derive a simple expression for k_{ex} in experiments on static quenching of luminescence described by three elementary reactions

$$A \rightarrow X, \qquad k_1, \qquad (60)$$
$$X \rightarrow A, \qquad k_2, \qquad (61)$$

and reaction (57)

$$X + Y \rightarrow A + Y, \qquad k_3,$$

which proceed only in water nanodroplets of a microemulsion. The rate constant corresponding to reaction (60) is proportional to the intensity of illumination, while reaction (61) represents all monomolecular processes quenching the excited state. The intensity I of luminescence is proportional to the steady-state concentration $[X]_{SS}$ of particles X, so that

$$\frac{I}{I_B} = \frac{[X]_{SS}}{[X]_B},$$

where I_B is the intensity of luminescence in the absence of quencher, and $[X]_B = k_1[A]/k_2$.

Figure 14 shows the dependencies of $\langle n_X \rangle_{SS}$ on k_{ex}/k_2 obtained by the PCA method at various parameters of the model (57), (60), (61), where $\langle n_X \rangle_{SS}$ is the averaged number of particles in a cell determined by (15) such that $\langle n_X \rangle_{SS}/(V_m N_A) = [X]_{SS}$. Mathematical treatment of these data reveals that the dependencies obtained are ideally described by a simple expression which, being solved with
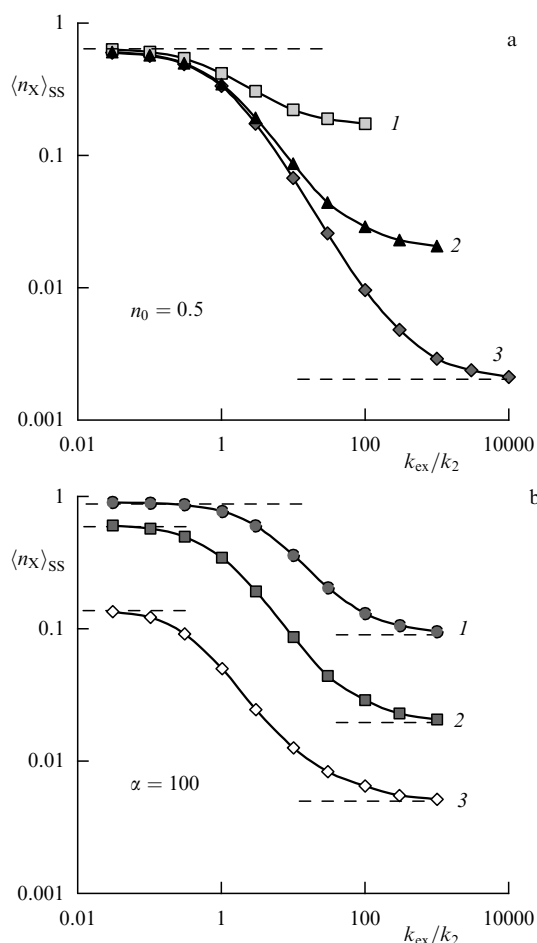
Figure 14. Dependencies of $\langle n_X \rangle_{SS}$ on k_{ex}/k_2 obtained by the PCA method at $n_0 = 0.5$ (a) and $\alpha = 100$ (b). The model parameters are $k_1[A]V_m N_A = k_2 = 1$; (a) $k'_3 = 10$ (curve *1*), $k'_3 = 100$ (curve *2*), $k'_3 = 1000$ (curve *3*); (b) $n_0 = 0.1$ (curve *1*), $n_0 = 0.5$ (curve *2*), $n_0 = 2$ (curve *3*). The maximum and minimum for each curve are depicted by dashed lines corresponding to (63).

respect to k_{ex}, has the form

$$k_{ex} = f(n_0)k_2 \, \frac{I_{max}/I_B - I/I_B}{I/I_B - I_{min}/I_B} \, , \qquad (62)$$

where

$$\frac{I_{max}}{I_B} = \exp(-n_0) + \frac{S_1(n_0)}{\alpha} \, , \qquad \frac{I_{min}}{I_B} = \frac{1}{1 + \alpha n_0} \, , \qquad (63)$$

$$\alpha \equiv \frac{k'_3}{k_2} \, , \qquad S_1(n_0) \equiv \sum_{n=1}^{\infty} \frac{P(n, n_0)}{n} \, , \qquad k'_3 \equiv k_r = \frac{k_3}{V_m N_A} \, ;$$

$f(n_0) \cong 5$ for $n_0 = 0.1$, $f(n_0) \cong 1.35$ for $n_0 = 0.5$, and $f(n_0) \cong 0.62$ for $n_0 = 2$, where $n_0 \equiv \langle n_Y \rangle$ is the averaged number of quencher particles in a nanodroplet. Formula (62) complements the Infelta–Tachiya equation for determining k_{ex}. The derivation of Eqn (62) testifies that the PCA method is promising for the study of chemical and photochemical reactions in organised molecular ensembles generally and in microemulsions in particular.

To sum up, the PCA method can describe all the specific features of the three types of elementary nonlinear reactions (22), (54), (25), and (57) such as fluctuation effects and

restricted mobility of particles. Below we will apply the PCA method to describe complicated spatially extended systems consisting of two or more elementary stages and having critical and bifurcation points.

8.3 Stirring effects in the activator–inhibitor system.

Let us consider the so-called stirring effects (SE) caused by nucleation in a homogeneous stirring solution [33, 151–153]. In Section 2 we considered these effects with the use of a simple CA which allowed us to describe qualitatively the main properties of SE. But using a simple CA, we got some rather exotic dependencies which are never observed in experiments. As for PCA, their application enables adequate description of SE. Phenomenologically, SE show up as an increase in the period and amplitude of concentration oscillations or as an increase in the inductive period T_{ind} of an autocatalytic reaction which takes place as the intensity of turbulent stirring enhances. Such effects were observed in the BZ [153], BR [152] reactions and in a chlorite-iodide system [151]. The simplest model to illustrate the stirring effects is the uncompleted Oregonator model [154]

$$Y + A \rightarrow X, \qquad k_1[A] \, , \qquad (64)$$
$$X + Y \rightarrow 0, \qquad k_2 \, , \qquad (65)$$
$$X + A \rightarrow 2X, \qquad k_3[A] \, , \qquad (66)$$
$$X + X \rightarrow 0, \qquad k_4 \, , \qquad (67)$$

where $X = HBrO_2$, $Y = Br^-$, $A = BrO_3^-$. The set (64)–(67) is similar to the set (3)–(6) and describes autocatalytical growth of the concentration of activator X in the presence of inhibitor Y. Reaction (67) terminating the growth of [X] does not play a significant role at the initial stage of autocatalysis, when the concentration of [X] is small. If the concentration of [Y] is less than the critical one

$$[Y]_{crit} = \frac{k_3[A]}{k_2} \qquad (68)$$

the autocatalysis starts and the concentration of [Y] decreases to zero, since reaction (65) is assumed to be fast. Reaction (64) is slow and restricts the rate at which [Y] approaches $[Y]_{crit}$ when $[Y] > [Y]_{crit}$. This reaction is equivalent to the combination of reactions (5) and (6) in the model (3)–(6). The basic parameters of the model (64)–(67) are

$$[A] = 0.1 \, M, \qquad k_1 = 0.1 \, M^{-1} \, s^{-1}, \qquad k_2 = 10^6 \, M^{-1} \, s^{-1},$$
$$k_3 = 100 \, M^{-1} \, s^{-1}, \qquad k_4 = 10^3 \, M^{-1} \, s^{-1},$$

which are rather close to actual parameters of the elementary stages of the BZ reaction.

Figure 15 shows typical kinetic curves obtained by the PCA method for averaged $\langle n_X \rangle$ at various intensities of stirring (Reynolds numbers) given by the relation [33]

$$Re = ck_{mix}^{1/2} \, , \qquad (69)$$

where c is a constant measured in $s^{1/2}$, and constant k_{mix} is determined by Eqn (42). For all the curves the initial concentrations were

$$[Y]_0 = 2 \times 10^{-5} \, M, \qquad [X]_0 = 0 \, ,$$

and the initial distribution of molecules Y over the cells was the Poissonian one. Figure 15 shows also the time dependence
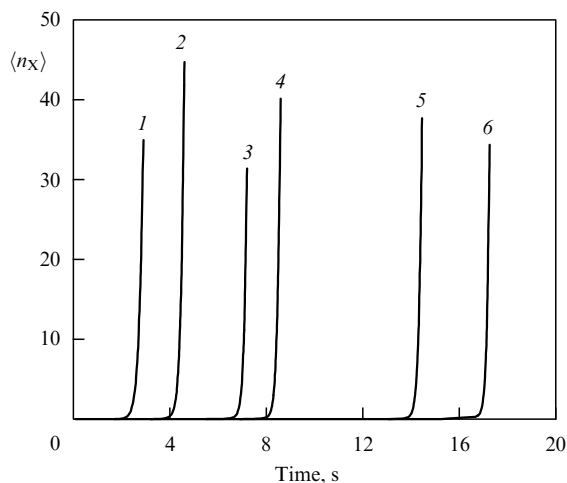
Figure 15. Time-dependencies of $\langle n_X \rangle$ at various Re and k_{ex}, obtained by the PCA method in simulating the set (64)–(67). The model parameters are $N \times N = 128 \times 128$, $V_m N_A = 5 \times 10^4$ M^{-1}, StepDif = 10^{-3} s, $\langle n_Y \rangle_0 = 1$, $\langle n_X \rangle_0 = 0$; $k_{ex} = 50$ s^{-1} (curves *1–4*), $k_{ex} = 1000$ s^{-1} (curve *5*); Re = 1.3 (for curve *1*), Re = 1.7 (*2*), Re = 2.57 (*3*), Re = 4.32 (*4*), Re = 1.46 (*5*) [33].

of [X] (as a product $[X] V_m N_A$, where $V_m N_A = 5 \times 10^4$ M^{-1}), obtained by solving ODE for the set (64)–(67) (curve *6*). Curve *6* can be compared with data found by the PCA method. As follows from Fig. 15 the induction period derived from these data is about $T_{ind} \cong 17$ s. As distinct from the one-parametric model considered in Section 2 with the use of a simple CA, the improved model can adequately represent the kinetics of decrease in the concentration of inhibitor Y in both an individual cell and the whole CA. Figure 16 presents some examples of these curves, which were used to determine T_{ind}.
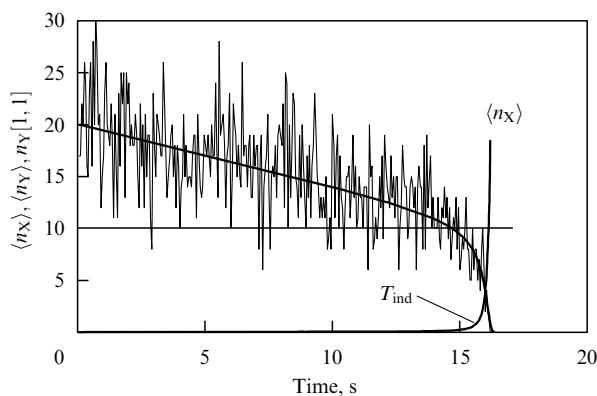

Figure 16. Kinetic curves of averaged concentrations $\langle n_X \rangle$ and $\langle n_Y \rangle$ (bold smooth curves) and values of $n_Y[1, 1]$ (fluctuactive curves) for a cell with coordinates [1, 1]. The horizontal line corresponds to the critical value $\langle n_Y \rangle_{cr} = 10$. The model parameters are $k_{ex} = 50$ s^{-1}, $V_m N_A = 1 \times 10^6$ M^{-1}, Re = 1.3, $\langle n_Y \rangle_0 = 20$ [33].

Figure 17 plots the dependencies of T_{ind} on Re at various $V_m N_A$ and k_{ex}, which have an S-like shape (curves *2*, *4–6*) similar to the experimental dependence [152]. For the values $V_m N_A$ and k_{ex} at which a pronounced stirring effect determined as the ratio $T_{in}^{max}/T_{ind}^{min}$ takes place (curves *2*, *4*, *5*) the product $k_{ex}(V_m)^{2/3}$ is constant $k_{ex}(V_m)^{2/3} \cong$ const $\cong D_0$. This means that the SE is determined by the molecular diffusion coefficient D_0, and, hence, depends on viscosity.
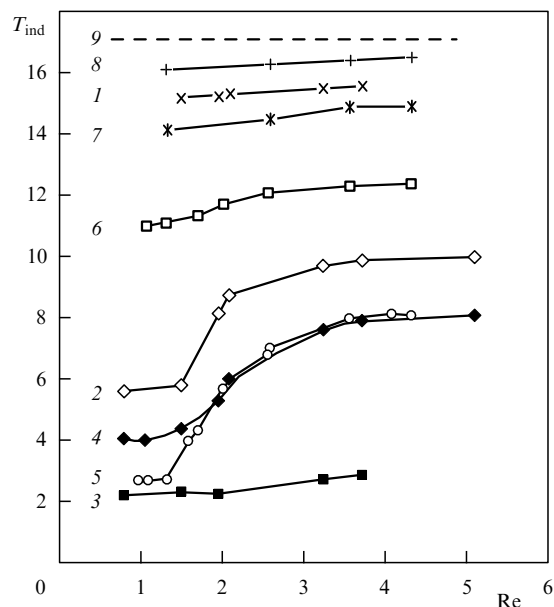

Figure 17. Dependencies of the induction period T_{ind} on the Reynolds number Re, obtained by the PCA in simulating the set (64)–(67). The model parameters are $k_{ex} = 20$ s^{-1} (for curves *1–3*), $k_{ex} = 50$ s^{-1} (for curves *4*, *5*, *8*), $k_{ex} = 200$ s^{-1} (curve *6*), $k_{ex} = 1000$ s^{-1} (curve *7*), $N_0 = 64^2$ (curves *1–4*), $N_0 = 128^2$ (curves *5–8*), $V_m N_A = 10^6$ M^{-1} (curves *1*, *8*), $V_m N_A = 2 \times 10^5$ M^{-1} (curve *2*), $V_m N_A = 5 \times 10^4$ M^{-1} (curves *3–7*). Curve *9* corresponds to the theoretical limit $T_{ind} = 17$ s obtained by numerical solution of the ODE for the set (64)–(67) with the parameters described above in the text [33].

The PCA method allows us to reveal the correlation between the SE and the total number of cells N_0 in the lattice. Let us compare the curves *4* ($N_0 = 64^2$) and *5* ($N_0 = 128^2$) in Fig. 17. The maximum of T_{ind} hardly changes (Re = 4–5), while the minimum of T_{ind} decreases by the factor 1.4 (at Re $\cong$ 1) as the number N_0 of cells grows. This result is very interesting. It is known that fluctuations or noise caused by discrete interactions self-average and tend to zero as the number of cells grows. In our case we are dealing with quite the opposite effect. As N_0 increases, the probability of the appearance of large-scale fluctuations rises too. These fluctuations are localised in clusters consisting of neighbouring cells which can be called *nuclei*. According to computer simulations, the consequences of the appearance of large-scale critical fluctuations override the smoothing effect of the increase in the number of cells. The reason is that the number of molecules X in nuclei grows autocatalytically. Figure 18 shows the influence of the stirring effect on nuclei: the greater the intensity of stirring, the smaller the nuclei. At Re = 4.34 nuclei are not revealed (Fig. 18d).

The data obtained by the PCA method confirm the experimental evidence that the SE in the BZ reaction becomes more pronounced as the rate v_Y at which [Y] approaches the critical value $[Y]_{cr}$ decreases [153]. The rate v_Y was calculated from the slope of the initial linear portion of the time dependence of [Y] (see, for example curve $\langle n_Y \rangle$ in Fig. 16) and was controlled by the constant k_1. As is seen from Table 3, the slower the rate v_Y, the more pronounced the stirring effect. This is in agreement with the experimental data [153] and confirms the ability of the PCA method to explain stirring effects, i.e. its suitability for reaction–diffusion–convection problems with regard to fluctuations.
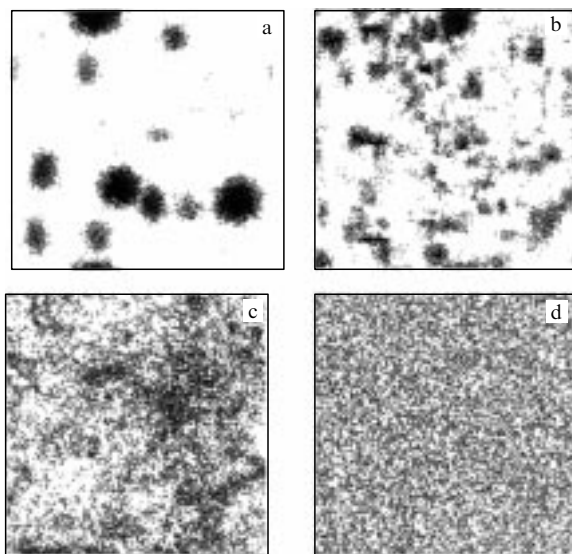
Figure 18. X-patterns for $\langle n_X \rangle = 3$ at various Reynolds numbers, obtained by the PCA method in simulating the set (64)–(67). The gray and black cells correspond to the states with $n_X \geqslant 2$. The model parameters are $N \times N = 128 \times 128$, $k_{ex} = 50$ s^{-1}, $V_m N_A = 5 \times 10^4$ M^{-1}, StepDif = 10^{-3} s, Re = 1.08 (a), Re = 1.57 (b), Re = 2.02 (c), Re = 4.34 (d) [33].

Table 3. Dependence of ratio $T_{ind}^{max} / T_{ind}^{min}$ (stirring effect) on the rate v_Y [1] at which the BZ system approaches the critical concentration $[Y_{cr}] = [A]k_3/k_2$ [2].

$[A]k_1$, s^{-1}	$100 v_Y / [Y]_0$, s^{-1}	T_{ind}^{min}, s [3]	T_{ind}^{max}, s	$T_{ind}^{max} / T_{ind}^{min}$
0.01	2.94	2.87	8.2	2.85
0.02	5.98	2.55	5.45	2.13
0.03	8.69	2.18	4.15	1.9
0.04	11.36	1.82	3.2	1.75

[1] The rates v_Y are obtained by numerical solution of the ODE for the set (64)–(67).

[2] $[Y]_0 = 2 \times 10^{-5}$ M, $[X]_0 = 0$, $[A] = 0.1$ M, $k_2 = 10^6$ M^{-1} s^{-1}, $k_3 = 100$ M^{-1} s^{-1}, $k_4 = 10^3$ M^{-1} s^{-1}.

[3] The values of maximum T_{ind}^{max} and minimum T_{ind}^{min} of the induction period are found by the PCA method at Re = 4 and Re = 1 respectively.

8.4 Coupled stochastic chemical oscillators

Let us consider the complete Oregonator model [154], which is the mathematical model of the oscillating BZ reaction. Modifying reaction (66) as

$$A + X \rightarrow 2X + 2Z \tag{70}$$

and adding the reaction

$$Z + B \rightarrow gY, \qquad k_5 \tag{71}$$

to the modified set (64)–(67), where B is malonic acid, whose concentration is rather high and constant, and g is the stoichiometric coefficient ($0 < g < 1$), we get the Oregonator model. Relaxation oscillations described by the model can be treated as a fast autocatalytic increase in the activator concentration X [reaction (70)] followed, after a delay, by a fast increase in the inhibitor concentration Y [reaction (71)] and a slow decrease in the inhibitor concentration to the critical value $[Y]_{cr}$ [reaction (64)].

In the previous section we showed that fluctuations (nuclei) decrease the induction period of autocatalysis

described by the set (64)–(67). In terms of the Oregonator model this means that fluctuations should decrease the oscillation period which is mainly determined by the induction interval. The fluctuations, in turn, can be controlled by mass-exchange rate constants k_X, k_Y, and k_Z. As the constants k_X, k_Y, or k_Z decrease the coupling strength between cells becomes weaker which enables us to consider each cell as a stochastic oscillator weakly coupled with neighbouring oscillators. The value V_m can be used to control the number of particles in an individual cell and, accordingly, the extent of the stochastic effect: the smaller the value V_m, the larger the amplitude of fluctuations. Thus, studying a spatially extended oscillating system, we naturally come to the problem of interacting stochastic oscillators. This point may be all the more evident if a cell of a CA is taken to mean inverted micelles or vesicles which are closed micro- or nanovolumes with semi-permeable membranes. The problem of interacting oscillators came under the scrutiny of science long ago and still attracts the attention of researchers [155–159]. In this section we consider the dependence of the oscillation period of the set of interacting stochastic oscillators described by the Oregonator model on the mass-exchange constants k_X, k_Y, k_Z.

The set of stochastic oscillators described by the Oregonator model [34] was mainly studied for a lattice of size 32×32 containing 1024 coupled stochastic elementary oscillators. There the following values for the rate constants of reactions (64), (65), (67), (70), and (71) were used:

$$k_1 = 0.2 \text{ M}^{-1} \text{s}^{-1}, \qquad k_2 = 2 \times 10^5 \text{ M}^{-1} \text{s}^{-1},$$

$$k_3 = 20 \text{ M}^{-1} \text{s}^{-1}, \qquad k_4 = 2 \times 10^3 \text{ M}^{-1} \text{s}^{-1},$$

$$k_5 = 1 \text{ M}^{-1} \text{s}^{-1}, \qquad [B] = 1 \text{ M}.$$

The activator concentration varied in the range from $[A] = 0.01$ M, up to $[A] = 1$ M. To describe reaction (71) by the PCA method we put $g = 0.5$ and treat reaction (71) as the process

$$n_Z \rightarrow n_Z - 2,$$
$$n_Y \rightarrow n_Y + 1, \tag{72}$$

which occurs with the probability $W_5 = k_5[B]\langle n_Z \rangle \tau / 2$ instead of the probability $W_5 = k_5[B]\langle n_Z \rangle \tau$. It turned out to be a good approximation, since at strong coupling between the cells the kinetic curves obtained by the PCA method coincide virtually with those found by numerical integration of the corresponding set of ODE of the model (64), (65), (67), (70), (71).

Characteristic kinetic curves for various k_X under condition of intensive stirring are shown in Fig. 19. At k_X, k_Y, and k_Z exceeding 30 s^{-1} the oscillating kinetic curves completely coincide with the curves obtained from the solution of the relevant ODE. As the rate constants k_X and k_Y ($k_X = k_Y$) decrease and at $k_Z = \text{const} = 32$ s^{-1}, the oscillation period and the amplitude also decrease, and the relaxation oscillations become sinusoidal.

Figure 20 plots the dependence of the oscillation period on the constant $k_X = k_Y$ at various $V_m N_A$. It is evident that as the constant k_X decreases and becomes less than the critical value k_{cr}, the period T flattens out and tends to the limiting value T_m. It is also seen that the smaller is $V_m N_A$, the shorter the limiting value T_m and the greater the ratio T_0/T_m, where T_0 is the limit at $k_X \rightarrow \infty$. In the vicinity of the critical constant k_{cr} the difference $T - T_m$ depends on the difference
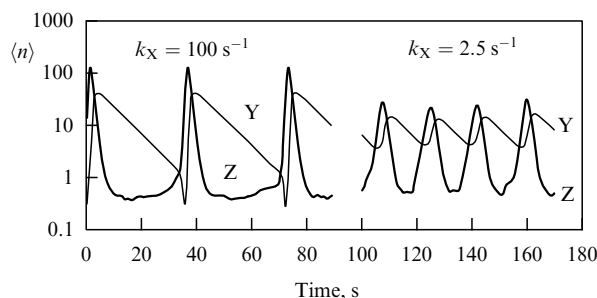
Figure 19. Oscillations of the averaged number of particles Y and Z obtained by the PCA method in simulating the stochastic Oregonator model at various mass-exchange constants $k_X = k_Y$ and $k_Z = 32 \text{ s}^{-1}$. The model parameters are $[A] = 0.3$ M, $V_m N_A = 4 \times 10^4$ M^{-1}, $N \times N = 32 \times 32$, StepMix $= 0.05$ s. The oscillation period is $T = 35$ s at $k_X = 100 \text{ s}^{-1}$ and $T = 17.5$ s at $k_X = 2.5 \text{ s}^{-1}$ [34].
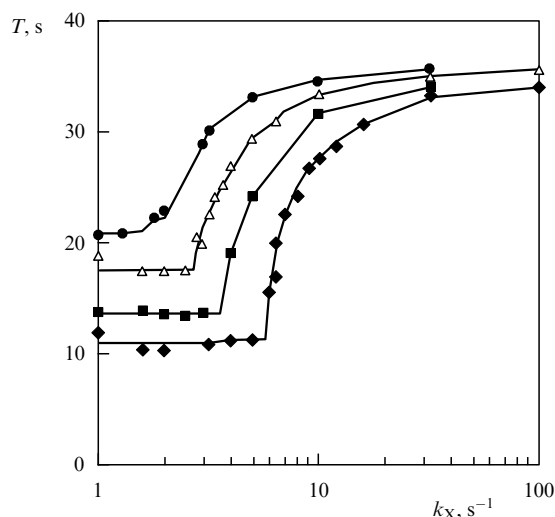

Figure 20. Dependence of the oscillation period on the mass-exchange constant k_X ($k_X = k_Y$), found for the stochastic Oregonator model at $[A] = 0.3$ M, $k_Z = 32 \text{ s}^{-1}$, $N \times N = 32 \times 32$, cells were stirred at time intervals StepMix $= 0.05$ s by random sampling of 8×8-sized squares performed 32 times and random rearrangement of their quadrants. The curves running from the top down correspond to the model parameters $V_m N_A = 1 \times 10^5, 4 \times 10^4, 2 \times 10^4, 1 \times 10^4 \text{ M}^{-1}$ [34].

$k_X - k_{cr}$ as

$$T - T_m \propto (k_X - k_{cr})^{1/2}.$$

Such a dependence of the order parameter on the controlling parameter is typical for second-order phase transitions.

A frequency multiplying bifurcation (not to be confused with the bifurcation of period doubling) was shown in Ref. [34] to take place as the strength of coupling between stochastic oscillator changes (mainly due to the change in the constant k_X). A specific feature of the bifurcation is that it depends on the microvolume size. The smaller the size, the greater the multiplier for the frequency of oscillations when the constant k_X decreases below the critical value k_{cr}. It was concluded that the effect results from the stochastic behaviour of elementary oscillators. If the concentration of particles X and, hence, particles Z begins to increase autocatalytically in an elementary oscillator (one of a huge number $N \times N$), then the oscillator, so to say, initiates a multiplication of particles in all the other elementary

oscillators, although the values n_Y have not decreased there to the critical one.

This multiplication of the frequency of oscillations can occur when the strength of coupling between elementary oscillators is neither too large nor too small. When the mass-exchange rate constant is high $k_{ex} \gg \gamma_i$, where γ_i is the *quasi*-first order rate constants for reactions (64), (65), (67), (70), (71), the stochastic behaviour of elementary oscillators is suppressed, they oscillate in phase. At low mass-exchange constant $k_{ex} \ll \gamma_i$, any coupling between elementary oscillators is lost, resulting in absolute chaos and the system as a single whole does not oscillate. The system is most sensitive to the strength of coupling at the critical value k_{cr}, where the mass-exchange constant k_X is of the order of the constant γ_3 for the exponential growth of the activator concentration, $\gamma_3 = k_3[A]$.

8.5 Other problems
In this review we have not considered the use of CA methods in many other problems, for example, in the study of fluctuation effects on positions of bifurcation points in a bistable system. The analysis of Turing structures and autowave phenomena in excitable media [160] also deserves special consideration. Extensive studies of heterogeneous catalysis and oscillatory and chaotic reactions on a catalyzer surface [161] have been left beyond the scope of the review. An interesting effect of synchronisation of the activity of enzymes in microvolumes was revealed by the CA method in the papers by B Hess and A Mikhaĭlov [162, 163]. A wide field of use of CA is self-organised criticality (see, for example, Refs [164, 165], as well as numerous papers in *Physical Review E*). In other words, the CA method has a wide area of application.

9. Conclusions

There are a lot of modifications to the CA method. Mathematicians deal mainly with simple CA, since the studies by these methods may involve interesting purely mathematical problems. Physicists and those specialised in chemical physics often use the LGCA, DSMC and PCA methods, since these methods enable them to describe fine details of the behaviour of actual systems at micro- and mesolevel, in particular, the influence of internal fluctuations on the behaviour of dynamical systems. Chemists prefer the CA-ODE (or CM) methods which rely on their habitual concept of concentration. Common to all the methods is the idea of local description of a spatially extended system. What is more, the methods coincide in the limiting cases. Table 4 lists the CA methods and their fields of application. It can serve as an illustration of the development of the methods. Table 4 does not pretend to be complete for simple or classical CA.

Advances in computer techniques stimulate the development of the CA methods. With a Pentium 200 type PC, one can calculate any of the above-discussed problems in a minute or a day, and it will take one a day or a week to obtain the dependencies revealing the nature of one or other effect. However, it is not only the speed of getting results which matters. Baras and Malek Mansur [15, 143, 108] believe the DSMC method and, hence, the LGCA and PCA methods are a unique tool to test the correctness of results found by the solution of the master equation, since they are based on the main principles of statistical physics.

Table 4. Various types of cellular automata [1] and their application.

Type of CA	Author, year of publication [Ref.]	Modelling
Finite automata	M L Tsetlin, 1961 [1, 2]	Advisable behaviour, self-correction
SCA	J von Neumann, 1966 [8]	Self-replication of organisms
SCA	W Keirstead, B A Huberman, 1986 [73, 74]	Crystal and cluster formation
SCA	Y Oono, M Kohmoto, 1987 [78]	Wave processes in the media of oscillating cells
SCA	V K Vanag, A Yu Virchenko, K V Vanag, A O Aït, 1996 [14, 79]	Stirring effects in BZ and BR reactions
SCA	A Deutsch, 1996 [19]	Cooperative motion of organisms
SCA	T Pöschel, J A Freund, 1997 [53]	'Free-motion – jam' transition in cities
CM	W Horsthemke, L Hannon, 1984 [88]; P Ruoff, 1993 [94]; J Hlavacova, P. Sevcik, 1994 [95]; F Ali, M Menzinger, 1997 [93]	Stirring effects in the BZ reaction
LGA	D d'Humières, 1990 [17, 18]; U Frisch, B. Hasslacher, Y Pomeau, 1986 [102]	Hydrodynamic problems
LGSA	R Kapral et al., 1990 – 1996 [22 – 25, 35, 46, 96, 98]	Reaction – diffusion equations with the account of fluctuations (chaos, chemical waves, Turing structures, nuclei formation, etc.)
DSMC	G A Bird, 1976, 1987 [109 – 111]; D T Gillespie, 1976 [119]; J S Turner, 1977 [121]; F Baras, M Malek Mansour, 1990 – 1997 [15, 43, 57, 106 – 108, 114]	Gas dynamics, master equation, chemical reactions with account of fluctuations
PCA	V K Vanag, 1996 – 1998 [33, 34, 50]	Reaction – diffusion equations with account of fluctuations and turbulent stirring in homogeneous and heterogeneous media

[1] SCA — simple or classical cellular automata, CM — cellular models, LGA — lattice gas automata, LGCA — lattice gas cellular automata, DSMC — Direct simulation Monte Carlo, PCA — probabilistic cellular automaton using the Monte Carlo procedure.

Nonlinear reactions in three-dimensional space including heterogeneous spatial systems of fractal dimensionality call for further investigation. We might expect the appearance of works where the CA would have the configuration of the studied object or a reactor and take account of incoming and outgoing fluxes, while the cells of CA would change during a reaction depending on the reagents, and the varied size of cells could, in turn, affect the probabilities of the processes occurring there.

References

1. Tsetlin M L *Dokl. Akad. Nauk USSR* **139** 830 (1961)
2. Tsetlin M L *Issledovaniya po Teorii Avtomatov i Modelirovaniyu Biologicheskikh Sistem* (Automaton Theory and Modeling of Biological Systems) (Moscow: Nauka, 1969) [Translated into English (New York: Academic Press, 1973)]
3. Kobrinskiĭ N E, Trakhtenbrot B A *Vvedenie v Teoriyu Konechnykh Avtomatov* (Introduction to the Theory of Finite Automata) (Moscow: Fizmatgiz, 1962) [Translated into English (Amsterdam: North-Holland Publ. Co., 1965)]
4. Glushkov V M *Sintez Tsifrovykh Avotmatov* (Synthesis of Digital Automata) (Moscow: Fizmatgiz, 1962)
5. Glushkov V M *Vvedenie v Teoriyu Samosovershenstvuyushchikhsya Sistem* (Introduction to the Theory of Self-Perfecting Systems) (Kiev: KVIRTU, 1962)
6. Tsetlin M L, Krylov V Yu *Dokl. Akad. Nauk USSR* **149** 284 (1963)
7. Krinskiĭ V I *Biofiz.* **9** 484 (1964)
8. von Neumann J *Theory of Self-Reproducing Automata* (Urbana: University of Illinois Press, 1966)
9. Wolfram S *Cellular Automata and Complexity* (New York: Addison-Wesley, 1994)
10. Wolfram S *Rev. Mod. Phys.* **55** 601 (1983)
11. Wolfram S *Theory and Applications of Cellular Automata* (Singapore: World Scientific, 1986)
12. Wolfram S *Physica D* **10** 1 (1984)
13. Loskutov A Yu, Mikhaĭlov A S *Vvedenie v Sinergetiku* (Introduction to Synergetics) (Moscow: Nauka, 1990)
14. Aït A O, Vanag V k *Zh. Fiz. Khim.* **70** 1385 (1996)
15. Baras F, Malek Mansour M, in *Advances in Chemical Physics,* Vol. 100 (Eds I Prigogine, S A Rice) (New York: Wiley, 1997) p. 393
16. Chou H-H, Reggia J A *Physica D* **110** 252 (1997)
17. d'Humières D, in *Cellular Automata and Modeling of Complex Physical Systems* (Springer Proceedings in Physics, Vol. 46, Eds P Manneville et al.) (Berlin: Springer-Verlag, 1990) p. 186
18. d'Humières D *Physica D* **47** 299 (1991)
19. Deutsch A *Int. J. Bifurcation and Chaos* **6** 1735 (1996)
20. Dow R A *Physica D* **110** 67 (1997)
21. Greeberg J M, Hastings S P *SIAM J. Appl. Math.* **34** 515 (1978)
22. Gruner D, Kapral R, Lawniczak A *J. Chem. Phys.* **99** 3938 (1993)
23. Kapral R, Lawniczak A, Masiar P *J. Chem. Phys.* **96** 2762 (1992)
24. Kapral R, Wu X-G, in *Chemical Waves and Patterns* (Eds R Kapral, K Showalter) (New York: Kluwer, 1995) p. 609
25. Kapral R, Wu X-G *J. Phys. Chem.* **100** 18976 (1996)
26. Markus M et al. *Int. J. Bifurcation and Chaos* **6** 1817 (1996)
27. Maselko J *J. Phys. Chem.* **99** 2949 (1995)
28. Moore C *Physica D* **111** 27 (1998)
29. Munuzuri A, Markus M *Int. J. Bifurcation and Chaos* **6** 1837 (1996)
30. Prakash S, Nicolis G *J. Stat. Phys.* **86** 1289 (1997)
31. Provata A, Turner J W, Nicolis G *J. Stat. Phys.* **70** 1195 (1998)
32. Stampfle M *Int. J. Bifurcation and Chaos* **6** 603 (1996)
33. Vanag V K *J. Phys. Chem.* **100** 11336 (1996)
34. Vanag V K *J. Phys. Chem. A* **101** 7074 (1997)
35. Wu X-G, Kapral R *J. Chem. Phys.* **100** 5936 (1994)
36. Bunimovich L A *Int. J. Bifurcation and Chaos* **6** 1127 (1996)
37. Durrett R *Nonlinear Science Today* **1** 1 (1991)
38. Durrett R, Griffeath D *J. Exp. Math.* **2** 183 (1993)
39. Fisch R, Gravner J, Griffeath D *Statistics and Computing* **1** 23 (1991)
40. Gravner J, Griffeath D *Trans. Am. Math. Soc.* **340** 837 (1993)
41. Gutowitz H *Complexity* **1** 16 (1996)
42. Gutowitz H *Complexity* **1** 29 (1996)
43. Baras F, Malek Mansour M *Phys. Rev. E* **54** 6139 (1996)
44. Brieger L, Bonomi E *Physica D* **47** 159 (1991)
45. Gerhardt M, Schuster H, Tyson J J *Science* **247** 1563 (1990)
46. Lawniczak A et al. *Physica D* **47** 132 (1991)
47. Markus M, Hess B *Nature* (London) **347** 56 (1990)
48. Prakash S, Nicolis G *J. Stat. Phys.* **82** 297 (1996)
49. Schepers H E, Markus M *Physica A* **188** 337 (1992)
50. Vanag V K, Nicolis G *J.Chem. Phys.* (in press)
51. Gutowitz H, in *Cellular Automata and Cooperative Phenomena* (Eds E Goles, N Boccara) (New York: Kluwer, 1993)
52. Chen S et al. *Physica D* **47** 97 (1991)
53. Pöschel T, Freund J A, in *Stochastic Dynamics* (Eds L Schimansky-Geier, T Poschel) (Berlin: Springer, 1997) p. 220

54. Meinhardt H *Int. J. Bifurcation and Chaos* **7** 1 (1997)
55. Klimontovich Yu L *Usp. Fiz. Nauk* **164** 811 (1994) [*Phys. Usp.* **37** 737 (1994)]
56. Alexander S et al. *Rev. Mod. Phys.* **53** 175 (1981)
57. Baras F *Phys. Rev. Lett.* **77** 1398 (1996)
58. Havlin S, Ben-Avraham D *Adv. Phys.* **36** 695 (1987)
59. Nicolis G, Prigogine I *Self-Organization in Nonequilibrium Systems* (New York: Wiley, 1977)
60. Nicolis G, Altares V *J. Phys. Chem.* **93** 2861 (1989)
61. Crutchfield J P, Hanson J E *Physica D* **69** 279 (1993)
62. Hardy J, Pomeau Y *J. Math. Phys.* **13** 1042 (1972)
63. Taguchi Y, Takayasu H *Physica D* **69** 366 (1993)
64. Domany E, Kinzel W *Phys. Rev. Lett.* **53** 311 (1984)
65. Kinzel W *Z. Phys. B* **58** 229 (1985)
66. Boissonade J *Phys. Lett. A* **74** 285 (1979)
67. Boissonade J *Physica A* **113** 607 (1982)
68. Ortoleva P, Yip S *J. Chem. Phys.* **65** 2045 (1976)
69. Chate H, Manneville P *Europhys. Lett.* **14** 409 (1991)
70. Langton C G *Physica D* **22** 120 (1986)
71. Langton C G, in *Emergent computation* (Ed. S Forrest) (Amsterdam: North-Holland, 1990) p. 12
72. Li W, Packard N H, Langton C G *Physica D* **45** 77 (1990)
73. Keirstead W, Huberman B A *Phys. Rev. Lett.* **56** 1094 (1986)
74. *Fractals in Physics* (Amsterdam: North-Holland, 1986)
75. Malinetskiĭ G G, Shakaeva M S *Dokl. Akad. Nauk USSR* **321** 711 (1991) [*Sov. Phys. Dokl.* **36** 826 (1991)]
76. Malinetskiĭ G G, Shakaeva M S *Dokl. Akad. Nauk USSR* **325** 716 (1992) [*Sov. Phys. Dokl.* **37** 401 (1992)]
77. Malinetskiĭ G G, Shakaeva M S *Zh. Fiz. Khim.* **69** 1523 (1995)
78. Oono Y, Kohmoto M *Phys. Rev. Lett.* **55** 2927 (1987)
79. Vanag V K, Virchenko A Yu, Vanag K V *Izv. Vyssh. Uchebn. Zaved. Prikladnaya Nelineĭnaya Dinamika* **4** (3) 97 (1996)
80. *Komp'yutery i Nelineĭnye Yavleniya: Informatika i Sovremennoe Estestvoznanie* (Computers and Nonlinear Phenomena: Informatics and Modern Science) (Ed. A A Samarskiĭ) (Moscow: Nauka, 1988)
81. Tachiya M, in *Kinetics of Nonhomogeneous Processes* (Ed. G R Freeman) (New York: Wiley, 1987) p. 575
82. Landau L D, Lifshits E M *Teoreticheskaya Fizika* Vol. 6 *Gidrodinamika* (Hydrodynamics) (Moscow: Nauka, 1988) [Translated into English (New York: Pergamon Press, 1990)]
83. Anacker L W, Kopelman R *Phys. Rev. Lett.* **58** 289 (1987)
84. Tretyakov A, Provata A, Nicolis G *J. Phys. Chem.* **99** 2770 (1995)
85. Curl R L *Am. Inst. Chem. Eng. J.* **9** 175 (1963)
86. Spielman L A, Levenspiel O *Chem. Eng. Sci.* **20** 247 (1965)
87. Evangelista J J, Katz S, Shinnar R *Am. Inst. Chem. Eng. J.* **15** 843 (1969)
88. Horsthemke W, Hannon L *J. Chem. Phys.* **81** 4363 (1984)
89. Chang P C, Mou C Y, Lee D J *Chem. Eng. Sci.* **51** 2601 (1996)
90. Fox R O, Erjaee G, Zou Q *Chem. Eng. Sci.* **49** 3465 (1994)
91. Lee D J, Chang P C, Mou C Y *J. Phys. Chem. A* **101** 1854 (1997)
92. Villermaux J *Rev. Chem. Eng.* **7** 51 (1991)
93. Ali F, Menzinger M *J. Phys. Chem. A* **101** 2304 (1997)
94. Ruoff P *J. Phys. Chem.* **97** 6405 (1993)
95. Hlavacova J, Sevcik P *J. Phys. Chem.* **98** 6304 (1994)
96. Dab D et al. *Phys. Rev. Lett.* **64** 2462 (1990)
97. Dab D, Boon J-P, Li Y-X *Phys. Rev. Lett.* **66** 2535 (1991)
98. Kapral R, Lawniczak A, Masiar P *Phys. Rev. Lett.* **66** 2539 (1991)
99. *Lattice Gas Methods for Partial Differential Equations* (New York: Addison-Wesley, 1990)
100. Boghosian B M et al. *Phys. Rev. E* **55** 4137 (1997)
101. d'Humières D et al. *Complex Systems* **1** 648 (1987)
102. Frisch U, Hasslacher B, Pomeau Y *Phys. Rev. Lett.* **56** 1505 (1986)
103. Grosfils P, Boon J-P, Lallemand P *Phys. Rev. Lett.* **68** 1077 (1992)
104. Grosfils P et al. *Phys. Rev. E* **48** 2665 (1993)
105. Weimar J R et al. *Europhys. Lett.* **20** 627 (1992)
106. Baras F, Pearson J E, Malek Mansour M *J. Chem. Phys.* **93** 5747 (1990)
107. Baras F, Nicolis G, in *Microscopic Simulation of Complex Flows* (Ed. M Mareschal) (New York: Plenum, 1990)
108. Baras F, Malek Mansour M, Pearson J E *J. Chem. Phys.* **105** 8257 (1996)
109. Bird G A *Molecular Gas Dynamics* (Oxford: Clarendon, 1976)
110. Bird G A *Phys. Fluids* **30** 364 (1987)

111. Bird G A *Molecular Gas Dynamics and the Direct Simulation of Gas Flows* (Oxford: Clarendon, 1994)
112. Chenoweth D R, Paolucci S *Phys. Fluids* **28** 2365 (1985)
113. Garcia A L *Numerical Methods for Physics* (Englewood Cliffs, N.J.: Prentice Hall, 1994)
114. Geysermans P, Baras F *J. Chem. Phys.* **105** 1402 (1996)
115. Mareschal M, De Wit A *J. Chem. Phys.* **96** 2000 (1992)
116. Muntz E P *Annu. Rev. Mech.* **21** 387 (1989)
117. Romanovskiĭ Yu M, Stepanova N V, Chernavskiĭ D S, in *Matematicheskoe Modelirovanie v Biofizike* (Mathematical Modelling in Biophysics) (Moscow: Nauka, 1975)
118. Klimontovich Yu L *Turbulentnoe Dvizhenie i Struktura Khaosa* (Turbulent Motion and the Structure of Chaos) (Moscow: Nauka, 1990) [Translated into English (Dordrecht: Kluwer Acad. Publ., 1991)]
119. Gillespie D T *J. Comput. Phys.* **22** 403 (1976)
120. Gillespie D T *J. Phys. Chem.* **81** 2340 (1977)
121. Turner J S *J. Phys. Chem.* **81** 2379 (1977)
122. Bunker D L et al. *III, Combust. Flame* **23** 373 (1974)
123. Nakanishi T *J. Phys. Soc. Jpn.* **32** 1313 (1972)
124. Nakanishi T *J. Phys. Soc. Jpn.* **40** 1232 (1976)
125. Aronovitz J A, Nelson D R *Phys. Rev. A* **29** 2012 (1984)
126. Almgren M, in *Kinetics and Catalysis in Microheterogeneous Systems* (Eds M Gratzel, K Kalyanasundaram) (New York: Dekker, 1991) p. 63
127. Koper G J M et al. *J. Phys. Chem.* **99** 13291 (1995)
128. Daniels F, Alberty R A *Physical Chemistry* 2nd ed. (New York: Wiley, 1975) [Translated into Russian (Moscow: Mir, 1978)]
129. Aguda B D, Clarke B L *J. Chem. Phys.* **89** 7428 (1988)
130. Willamowski K-D, Rössler O E *Z. Naturforsch. A* **35** 317 (1980)
131. Horsthemke W, Lefever R *Noise-Induced Transitions* (Berlin: Springer-Verlag, 1984) [Translated into Russian (Moscow: Mir, 1987)]
132. Deering W D, West B J *J. Stat. Phys.* **65** 1247 (1991)
133. Ovchinnikov A A, Zel'dovich Ya B *Khim. Fiz.* **28** 215 (1978)
134. Lin A L, Kopelman R, Argyrakis P *J. Phys. Chem. A* **101** 802 (1997)
135. Molski A, Bergling S, Keizer J *J. Phys. Chem.* **100** 19049 (1996)
136. Noyes R M, Gardiner W C (Jr) *J. Phys. Chem.* **85** 594 (1981)
137. Oshanin G et al. *J. Phys. Chem.* **98** 7390 (1994)
138. Reigada R et al. *J. Chem. Phys.* **105** 10925 (1996)
139. Reigada R et al. *J. Chem. Phys.* **107** 843 (1997)
140. Sancho J M et al. *J. Phys. Chem.* **100** 19066 (1996)
141. Sokolov I M, Argyrakis P, Blumen A *J. Phys. Chem.* **98** 7256 (1994)
142. Toussaint D, Wilczek F *J. Chem. Phys.* **78** 2642 (1983)
143. Burlatskiĭ S F, Ovchinnikov A A *Zh. Teor. Eksp. Fiz.* **92** 1618 (1987) [*Sov. Phys. JETP* **65** 908 (1987)]
144. Kopelman R *Science* **241** 1620 (1988)
145. Infelta P P, Gratzel M, Thomas J K *J. Phys. Chem.* **78** 190 (1974)
146. Tachiya M *Chem. Phys. Lett.* **33** 289 (1975)
147. Lianos P, Argyrakis P *J. Phys. Chem.* **98** 7278 (1994)
148. Almgren M, Johannsson R *J. Phys. Chem.* **96** 9512 (1992)
149. Almgren M, Johannsson R, Eriksson J C *J. Phys. Chem.* **97** 8590 (1993)
150. Johannsson R, Almgren M, Alsins J *J. Phys. Chem.* **95** 3819 (1991)
151. Epstein I R *Nature* (London) **374** 321 (1995)
152. Vanag V K, Alfimov M V *J. Phys. Chem.* **97** 1884 (1993)
153. Vanag V K, Melikhov D P *J. Phys. Chem.* **99** 17372 (1995)
154. Troy W, in *Oscillations and Travelling Waves in Chemical Systems* (Eds R Field, M Burger) (New York: Wiley, 1985) [Translated into Russian (Moscow: Mir, 1988) p. 167]
155. Astakhov V V et al. *Physica D* **109** 11 (1997)
156. Abarbanel' G D et al. *Usp. Fiz. Nauk* **166** 363 (1996) [*Phys. Usp.* **39** 337 (1996)]
157. Daido H *Int. J. Bifurcation and Chaos* **7** 807 (1997)
158. Han S K et al. *Int. J. Bifurcation and Chaos* **7** 877 (1997)
159. Kuramoto Y *Int. J. Bifurcation and Chaos* **7** 789 (1997)
160. Ivanitskiĭ G R, Medvinskiĭ A B, Tsyganov M A *Usp. Fiz. Nauk* **164** 1041 (1994)] [*Phys. Usp.* **37** 991 (1994)]
161. Mertens F, Imbihl R, Mikhailov A S *J. Chem. Phys.* **101** 9903 (1994)
162. Hess B, Mikhailov A S *Ber. Bunsenges. Phys. Chem.* **98** 1198 (1994)
163. Mikhailov A S, Hess B *J. Phys. Chem.* **100** 19059 (1996)
164. Bak P, Boettcher S *Physica D* **107** 143 (1997)
165. Newman M E J *Physica D* **107** 293 (1997)